INVESTIGATION OF EFFECTS OF NOVEL SELENIUM NANOPARTICLES FUNCTIONALIZED WITH *CORDYCEPS SINENSIS* ON OSTEOBLASTOGENESIS

CHAN CHEUK HIN

MPhil

The Hong Kong Polytechnic University

2018

The Hong Kong Polytechnic University

Department of Applied Biology and Chemical Technology

Investigation of Effects of Novel Selenium

Nanoparticles Functionalized with *Cordyceps sinensis*

on Osteoblastogenesis

CHAN CHEUK HIN

A thesis submitted in partial fulfilment of the requirements for the degree

of Master of Philosophy

July 2017

CERTIFICATE OF ORIGINALITY

I hereby declare that this thesis is my own work and that, to the best of my knowledge

and belief, it reproduces no material previously published or written, nor material that

has been accepted for the award of any other degree or diploma, except where due

acknowledgement has been made in the text.

                                     _____ (Signature)

CHAN CHEUK HIN (Name of Student)

26 June 2018 (Date)

ABSTRACT

Osteoporosis is a skeletal disease characterized by low bone mass and density as well as deterioration in bone microarchitecture, leading to high risk of bone fracture. With an increase in aging population, osteoporosis has become one of the major public health issues nowadays, causing significant medical and socioeconomic burdens.

Selenium is an essential trace mineral to human health. Substantial evidences have demonstrated that selenium deficiency is detrimental to bone microarchitecture and even associated with osteoporosis, suggesting its crucial role in bone metabolism. Recently, selenium nanoparticles (SeNPs) have become the new research target, since they were found to possess relatively low toxicity and remarkable anti-tumor efficacy compared to other organic and inorganic selenocompounds. Nevertheless, scientific research concerning their effects on bone health is currently very limited.

By using our patented nanotechnology [US patent no.: 9,072,669], our research team has successfully prepared novel SeNPs (Cs4-SeNPs) using the mushroom polysaccharide isolated from *Cordyceps sinensis*. We discovered that Cs4-SeNPs existed as well-dispensed spherical particles in water with an average diameter of 73.2 $\pm$ 3.49nm and was highly stable without significant increase in size after 6 weeks under 4°C. Further characterization using TEM also showed that the particle size of SeNPs in

Cs4-SeNPs was around 30nm. For individual SeNP, the clear lattice fringes (3.35Å), SAED pattern as well as EDX spectrum obtained by HR-TEM-EDX collectively indicated that the resulting nanoparticle possessed a polycrystalline structure with high level of Se (83.9%), implying a successfully fabrication of SeNPs using mushroom polysaccharides.

Endocytosis has been widely reported as the major cellular uptake mechanism for nanoparticles. Our study found that coumarin-6 labelled Cs4-SeNPs mainly localized in lysosomes of the murine preosteoblast MC3T3-E1 subclone 4 cells (bone forming progenitor cells) as early as 12 min after cellular internalization. Besides, substantial previous findings have demonstrated that promoting bone formation is one of the effective strategies to prevent and/or manage postmenopausal osteoporosis. Unlike the common food source of organic (e.g. selenomethionine) and inorganic selenocompounds (e.g. selenite), our study indicated that Cs4-SeNPs was found to exhibit a significant dose-dependent proliferation effect (range from 1.35 – 1.45 folds) on the MC3T3-E1 cells for 24, 48 and 72 hrs with the most effect dosage of 10μM. More importantly, Cs4-SeNPs (10μM) were found to markedly induce both osteoblast differentiation and bone mineral formation of the MC3T3-E1 cells as evidenced by a significant increase in ALP activity (3.05 ± 0.15 folds), as well as an enhancement of bone nodule formation (Von Kossa and Alizarin Red S staining). Further investigation

on their possible interaction with osteoclasts (bone resorption cells) also showed that Cs4-SeNPs could significantly up-regulate the gene expression ratio of the bone remodeling markers OPG/RANKL (2.56 ± 0.24 folds), suggesting their indirect inhibition effect on osteoclastogenesis in addition to promoting osteoblastogenesis.

Osteoblast differentiation is a crucial step of bone formation. Previous studies have demonstrated that BMP-2 signaling via Smad-dependent and/or Smad-independent pathway(s) is one of the most important signaling transduction cascades for regulating osteoblast differentiation. Interestingly, our study discovered that Cs4-SeNPs could trigger both BMP-2/Smad dependent and independent pathways simultaneously as evidenced by a significant upregulation of BMP-2 protein expression (1.46 ± 0.06 folds) as well as phosphorylation of Smad 1/5/8 (2.00 ± 0.25 folds) and p38 (1.60 ± 0.10 folds) proteins in the MC3T3-E1 cells after 3-day treatment. Besides, Cs4-SeNPs were found to significantly up-regulate the gene expression of those major downstream biomarkers in bone remodeling such as Dlx5 (1.71 ± 0.15 folds), Runx2 (1.48 ± 0.06 folds), Osx (1.46 ± 0.08 folds), ALP (1.77 ± 0.11 folds), and OCN (2.64 ± 0.14 folds), further supporting their active role in promotion of osteoblast differentiation and bone mineralization. Our long-term goal is to develop an evidence-based bone-forming agent for promoting the bone health of postmenopausal patients in our community.

<u>ACKNOWLEDGEMENTS</u>

This project requires large amount of research and work. With the support of many individuals, this project can conduct and complete smoothly. Therefore, I would like to thank for the following particulates.

First of all, I would like to thank for my supervisor Dr. Kahing Wong. Dr. Wong is pleasuring to provide guidance and help by spending time to discuss the project field and giving advises in improving for the experiment design.

In addition, I would like to thank our research team members, Dr. Chi-fai Wong, Dr. Peter Luk Kar Him and Mr. Cheung Siu To for providing technical support and expertise on this project. They are willing to provide superior knowledge, guidance and assistance for the projects.

CONTENTS

LIST OF FIGURES

LIST OF TABLES

LIST OF ABBREVIATION

AA   Ascorbic acid

ALP   Alkaline phosphatase

α-MEM   Alpha-Minimum essential medium

BCA   Bicinchoninic acid

BMP-2   Bone morphogenetic protein

CO2   Carbon dioxide

Cs4-SeNPs   *Cordyceps sinensis* selenium nanoparticles

DDI   Double deionized water

Dlx5   Distal-less homebox 5

DNA   Deoxyribonucleic acid

EDX   Electron dispersive X-ray spectroscopy

ERK   Extracellular receptor kinase

FBS   Fetal bovine serum

FT-IR   Fourier transform infrared

GAPDH   Glyceraldehyde 3-phosphate dehydrogenase

HRP   Horseradish peroxide

HRT   Hormonal replacement therapy

ICP-OES	Inductively coupled plasma optical emission spectrometry
IgG	Immunoglobulin G
JNK	c-Jun N-terminal kinases
KBr	Potassium bromide
MAPKs	Mitogen-activated protein kinase
MTS	3-(4,5-dimethylthiazol-2-yl)-5-(3-carboxymethoxyphenyl)-2-(4-sulfophenyl)-2H-tetrazolium
OCN	Oseocalcin
OPG	Osteoprotegerin
Osx	Osterix
PBS	Phosphate buffer saline
PMS	Phenazine methosulfate
pNPP	p-nitrophenyl phosphate
qPCR	Real time polymerase chain reaction
RANKL	Receptor activator of nuclear factor kappa-β ligand
RIPA	Radioimmunoprecipitation assay buffer
RNA	Ribonucleic acid
ROS	Reactive oxygen species
RT-PCR	Reverse transcription polymerase chain reaction

Runx2	Runt-related transcription factor 2
SAED	Selected area electron diffraction
SD	Standard deviation
SDS-PAGE	Sodium dodecyl sulfate
SEM	Standard error mean
SeNPs	Selenium nanoparticles
TBST	Tris-buffer saline with tween 20
TEM	Transmission electron microscopy

1. Introduction

1.1 <u>Osteoporosis</u>

Osteoporosis is a metabolic bone disease characterized by low bone mass as well as deterioration of bone micro-architecture, leading to high risk of bone fracture. In addition to elderly, postmenopausal woman is the major high-risk group of osteoporosis due to their loss of estrogen production. Estrogen is an important hormone regulating the turnover rate of bone tissue. Estrogen deficiency in postmenopausal woman would facilitate their osteoclasts formation and differentiation, enhancing bone resorption, hereby promoting loss of bone mineral density and deterioration of bone micro-architecture [1]. As reported by International Osteoporosis Foundation [2], osteoporosis is now influencing 200 million women worldwide, and bone fracture commonly occurred at body parts like hip, forearm and vertebrate. Subject to the increase of world aging population, osteoporosis has become one of the major public health issues nowadays, causing significant medical & socio-economical burdens. According to the Hospital Authority in Hong Kong, about 4,500 cases of hip fracture were reported annually, costing hospital expenditure around 52 million USD every year [3]. Due to the dramatic increase of Hong Kong's over 70-year-old population by 2050 [4], the cost on hip fracture related surgery and hospital care is expected to be increased significantly.

1.2 Current Medical Treatments for Osteoporosis

Bisphosphonate, denosumab and strontium ranelate are medical drugs currently used for treating and managing osteoporosis [4-14]. However, long-term consumption of these drugs has been found to associate with side effects such as hypocalcemia, serious allergic reaction, nausea, diarrhea and heart attack etc [14-19]. Hormone replacement therapy (HRT) has been widely used to alleviate the physical symptoms and to prevent clinical consequences of postmenopausal osteoporosis [20-21]. Similarly, recent studies by Women's Health Initiative as well as the Million Women reported that HRT would significantly increase the risk of postmenopausal women in developing breast cancer, stroke, thrombosis and cardiovascular disease [22-25]. Hence, there is a pressing need to develop alternative approach for managing and/or preventing postmenopausal osteoporosis.

1.3 Bone Remodeling

Bone remodeling is a lifelong process of regulating "new bone formation" and "old bone resorption". These two sub-processes are governed by specialized cell types called "osteoblast" and "osteoclast", respectively. During bone remodeling, osteoclasts will firstly carry out bone resorption by acidification and proteolytic digestion after

surface attachment of targeted regions. Then osteoblasts will secrete osteoid and form

secondary osteon at the resorbed regions followed by mineralization. Both osteoblasts

and osteoclasts play important roles in the bone remodeling cycle, and an imbalance of

which results in metabolic bone diseases like osteoporosis [26]. Substantial evidences

have demonstrated that promoting bone formation is one of effective strategies to

reduce the risk of first and recurrent fractures. Hence, there is a clear clinical need to

develop new bone forming agents for the prevention and treatment of postmenopausal

osteoporosis.

1.4 <u>Osteoblastic Differentiation</u>

Osteoblasts are derived from mesenchymal stem cells, which are also progenitors

of myocytes, chondrocytes and adipocytes [27]. During osteoblastogenesis, osteoblast

differentiation is one of the crucial steps (**Figure 1.** Osteoblastogenesis [Adopted from

[29]]). Substantial evidences have demonstrated that BMP-2 (bone morphogenetic

protein-2) signaling via Smad-dependent and/or Smad-independent pathway(s) is one

the most important signaling transduction cascades for regulating osteoblast

differentiation [28].

Normal osteoblast differentiation
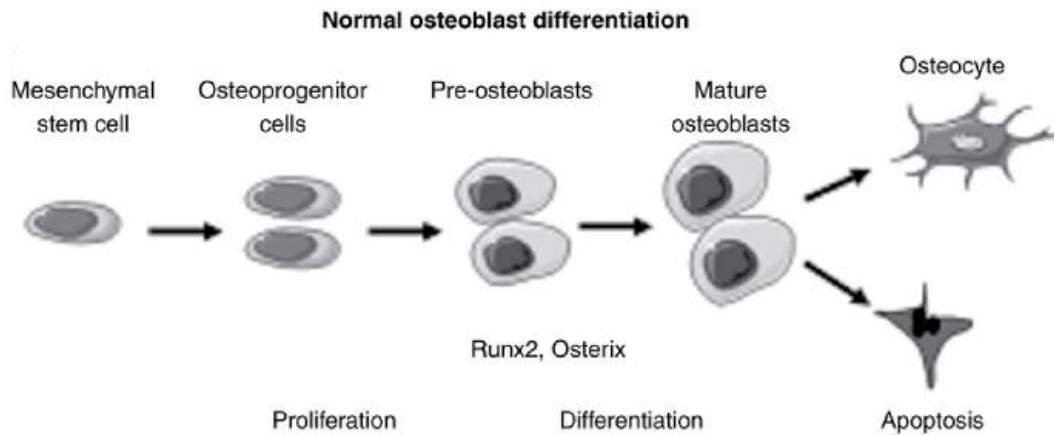
Figure 1. Osteoblastogenesis [Adopted from [29]]

1.4.1 BMP-2 signaling

BMPs are a group of phylogenetically conserved signaling molecules showed potent osteogenic effects and were initially identified by their capacity to induce endochondral bone formation [30-32]. BMP-2, -4 and -6 are the most readily detectable BMPs in osteoblast cultures [30, 33]. Different BMPs have their own unique functions in osteoblast differentiation. BMP-2, BMP-6, BMP-7 and BMP-9 have been found to promote bone formation, while BMP-3 acts as an inhibitor [34].

As shown in **Figure 2**, on receptor activation, BMP-2 transmit signals through Smad-dependent and/or Smad-independent pathways [35]. In Smad-dependent pathways, three classes of Smads are involved: (i) Receptor-regulated Smads (R-Smads), which are activated by Smad 1, 5 and 8; (ii) Common partner BMP mediator Smads (Co-

Smads) such as Smad 4; and (iii) Inhibitory Smads (I-Smads) such as Smad 6 and 7.

Upon ligand stimulation and activation by type II receptors, type I receptors

phosphorylate R-Smad followed by forming complexes with Co-Smads [36]. The R-

Smad/Co-Smads complexes will then translocate into the nucleus, regulating the

transcription of target genes by interacting with various transcription factors and

transcriptional coactivators or co-repressors. I-Smads will negatively regulate signaling

by the R-Smads and Co-Smads. Upon BMP-2 signaling activation, R-Smads and

Runx2 physically interact with each other and co-operatively regulate the transcription

of target genes, leading to osteoblast differentiation of mesenchymal progenitor cells [37-

39]. Interestingly, through the action of R-Smads, BMP does not induce the Runx2

expression in the mesenchymal progenitor cells directly. Instead, it facilitates the

expression of Dlx5 [40-41], which will then indirectly promote the Runx2 expression in

osteoprogenitor cells. Previous studies also discovered that transcription factors

including Hey1 (also termed HesR1 and Herp2), Tcf7, ITF-2, and ICSBP were

specifically expressed in osteoblast cells by BMP-2 treatment, involving both Notch

and Wnt signaling [42-43].

In Smad-independent pathway, BMP-2 has been reported to activate MAP kinases such as ERK, JNK and p38 in osteoblastic cells, regulating alkaline phosphatase (ALP) and osteocalcin (OCN) expressions [44-45]. It is worth noting that BMP-2 was found to activate JNK and p38 via protein kinase D (PKD) during osteoblastic differentiation, independent of protein kinase C (PKC) activity [46]. Previous studies also reported that Smad and p38 MAPK pathways converged at the Runx2 to regulate cell differentiation [47] and Runx2 plays a central role in the BMP-2-induced differentiation of C2C12 cells, diverting them from myogenic to osteogenic pathway [48-49]. Similar to Smad-dependent pathway, the homeobox gene Dlx5 is an upstream target of Smad-independent pathway, stimulating the downstream transcription factor, Runx2 followed by upregulating bone-specific genes during osteoblastic differentiation [41]. In addition to Runx2, BMP-2 has been found to promote osterix (Osx) expression in mouse progenitor cells and chondrocytes mediated by Dlx5 but is independent of Runx2 [50-52]. Interestingly, this BMP-2 inducing effect was mediated via p38 but not via ERK. Nevertheless, under osteogenic culture conditions, both ERK and p38 were involved in mediating the Osx expression [53].
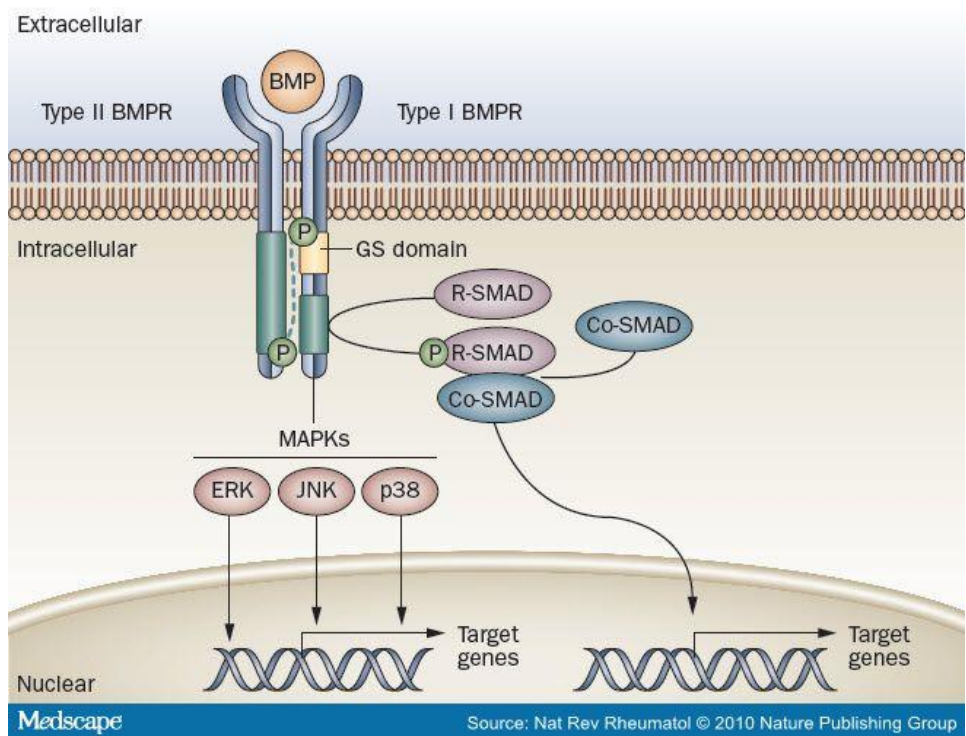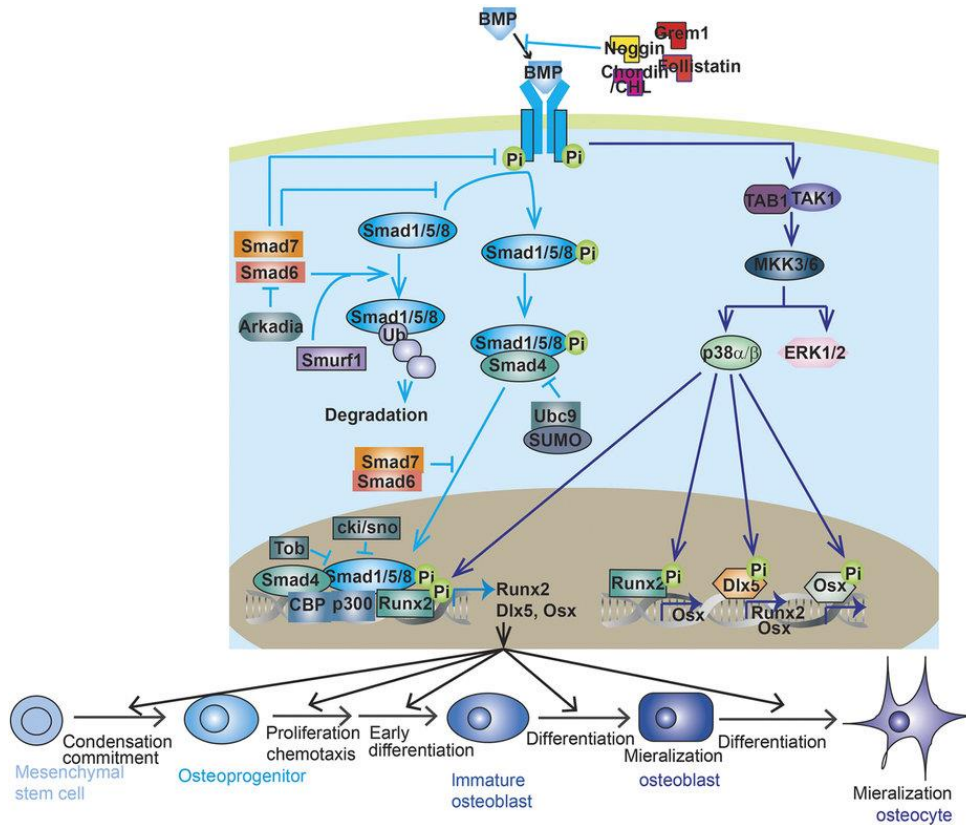
Figure 2. BMP-2 signaling pathway [54-55]

1.5 Selenium

Selenium (Se) is an essential trace mineral to human health [56]. Physiologically, Se is an important constituent of selenoproteins (e.g. thioredoxin reductase), which are important anti-oxidant enzymes to help protect the body from cellular damage by free radicals, supporting our immune system, cell proliferation and differentiation.[57-60]. According to USDA, the recommended daily intake of Se for adult is 55µg/day. For daily Se intake level above 400µg/day or below 40µg/day, it is considered to be "toxic" or "deficiency", respectively [61]. In the past decades, substantial evidences have demonstrated that Se deficiency is detrimental to bone micro-architecture and associated with osteopenia, osteoporosis as well as Kashin-Beck osteoarthropathy [58, 62-63], suggesting its crucial role in bone metabolism. Previous studies also indicated that Se supplementation could not only restore the anti-oxidative capacity and prevent cell damage in bone marrow stromal cells, but also protect their osteoblastic differentiation inhibited by H_2O_2 via suppressing oxidative stress and ERK signaling pathway [64].

The efficacy and toxicity of Se are highly dependent on its chemical form and dosage. Recently, Se nanoparticles (SeNPs) have become the new research target, since they were found to possess remarkable anti-cancer efficacy and low toxicity [65-66] compared to commom food source of organic and inorganic selenocompounds. Apart

from toxicity evaluation [67-68] as well as chemical and bio-synthesis [69-70], the *in vitro* anti-tumor efficacy of SeNPs have been widely reported in literature for the past ten years [71-73]. Although SeNPs stabilized with glutathione and bovine serum albumin have been recently found to promote the growth of primary human calvarial osteoblasts and alleviate the bone loss in ovariectomized rats, scientific research concerning the effects of SeNPs on bone health is still very limited. Besides, SeNPs aggregate easily and their health-promoting effects will be significantly reduced, once their nano size could not be maintained. This limiting factor has attracted many scientists to search for novel biomolecules that could stabilize the SeNPs without compromising their health-promoting effects.

1.6 *Cordyceps sinensis*

Cordyceps sinensis (Berk.) Sacc. (also called "Dong Chong Xia Cao" in China), which is a parasitic fungus on moth larvae of *Lepidoptera* (**Figure 3**), is a precious traditional Chinese medicine mainly distributed in Himalayas around Tibet and Nepal at altitudes of over 3,000 meters [6]. This caterpillar fungus has been used as a prestigious tonic and therapeutic herb in China for more than 700 years and has been listed as herbal drug in the official Chinese Pharmacopoeia by the Committee of Pharmacopoeia and Chinese Ministry of Health since 1964 [7]. As wild *C. sinensis* fruiting body-caterpillar

complexes are very rare and expensive, successfully cultivation of its 4th isolated mycelia (Cs4) by Chinese Academy of Sciences has undoubtedly facilitated both commercial production as well as scientific research in the past 20 years on this special strain [74]. Substantial pharmacological and clinical studies have demonstrated that polysaccharides are one of the major bioactive constituents of Cs4, which were found to exhibit a wide range of health-promoting and therapeutic effects such as immune-modulation, anti-tumor, anti-aging, anti-oxidant, hypoglycemia, hyperlipidaemia, and more importantly, bone protection in both cell and animal models [7-10]. Thus, it would be valuable to find out whether Cs4 polysaccharides could be used as capping agent to prepare novel SeNPs followed by investigating their effects on osteoblastogenesis.
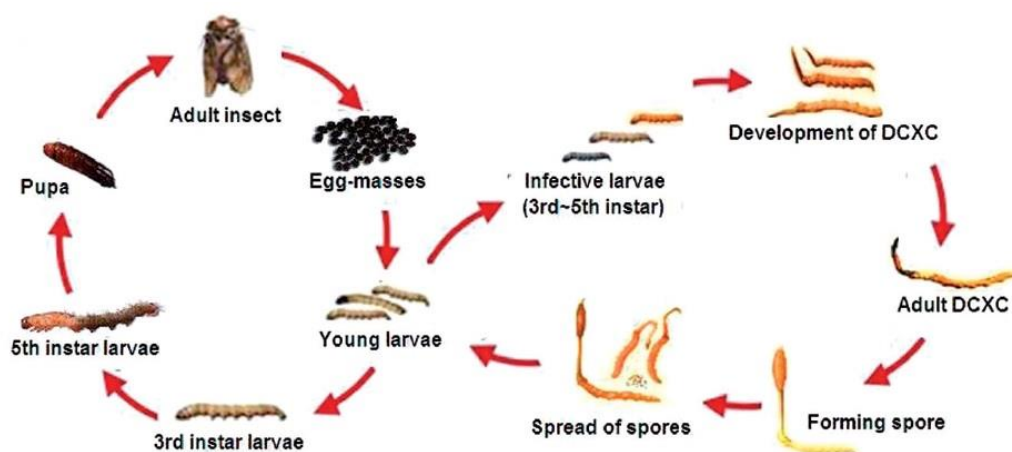
Figure 3. Life cycle of Lepidoptera and development of *Cordyceps sinensis* [75]

With a view to facilitating the development of Cs4-SeNPs into a novel bone

forming agent for prevention and treatment of osteoporosis, in this project, novel

selenium nanoparticles (Cs4-SeNPs) was prepared using the mushroom

polysaccharides isolated from *C. sinensis* followed by structure characterization.

Compared with the common food source of organic (e.g. selenomethionine) and

inorganic selenocompounds (e.g. selenite), their direct osteogenic effects on

preosteoblast murine MC3T3-E1 cells were evaluated. Apart from cellular uptake

behavior, the BMP signaling (both Smad-dependent and Smad-independent pathway)

modulated by Cs4-SeNPs during osteoblast differentiation will also be investigated. A

project summary is shown in **Figure 4**.

1.7 Hypothesis

a) Novel selenium nanoparticles (Cs4-SeNPs) could be prepared by using the

mushroom polysaccharides isolated from *Cordyceps sinensis*.

b) Cs4-SeNPs could induce osteoblastogenesis of murine preosteoblast MC3T3-E1

cells via BMP-2 signaling cascades

c) Cs4-SeNPs would enter the MC3T3-E1 cells via endocytosis

1.8 <u>Objectives</u>

a) To prepare and characterize novel selenium nanoparticles (Cs4-SeNPs) by using the

    mushroom polysaccharides isolated from *Cordyceps sinensis*

b) To characterize the direct effects of Cs4-SeNPs on osteoblastogenesis using

    preosteoblast MC3T3-E1 cells

c) To investigate the BMP signaling cascades modulated by Cs4-SeNPs during

    osteoblast differentiation using MC3T3-E1 cells

d) To study the cellular uptake behavior of Cs4-SeNPs by the MC3T3-E1 cells

1.9 <u>Experimental Design</u>

1.9.1 To prepare and characterize Cs4-SeNPs

According to our patented nanotechnology (US patent no.: 9,072,669), standardized

Cs4-SeNPs (Se concentration: 1.35 ± 0.12 mM) were prepared by using the water-

soluble polysaccharides isolated from *Cordyceps sinensis*. Structure and composition

of Cs4-SeNPs were further characterized by Nanosight NS300, TEM (Hitachi H-7650),

HR-TEM-EDX (JEOL 2010 + Horiba EX-250), and FT-IR (Bruker Equinox 55).

1.9.2 To investigate the direct effects of Cs4-SeNPs on osteoblastogenesis in vitro

Preosteoblast murine MC3T3-E1 subclone 4 cells (ATCC; CRL-2593) is one of *in vitro* models widely used for studying osteoblastogenesis [76], since they are able to exhibit phenotypic differentiation from pre-osteoblast to osteoblast under the induction of ascorbic acid (AA) and beta-glyverophosphate [77-79]. In this study, a dose- and time-dependent study of the osteogenic effect of Cs4-SeNPs (including cell proliferation, osteoblast differentiation and bone mineral formation) on MC3T3-E1 cells was performed. The effective dosage of Cs4-SeNPs for the MC3T3-E1 cells was firstly determined and then applied in the time-dependent studies.

1.9.3 To elucidate the mechanism of action of Cs4-SeNPs on osteoblastogenesis in vitro

Substantial evidences have demonstrated that BMP-2 signaling via Smad-dependent and/or Smad-independent pathway(s) is one the most important signaling cascades in regulating osteoblastogenesis [28]. Upon cell surface ligand binding, BMP-2 forms a hetero-tetrameric receptor complex with the dimers of both type II and type I transmembrane serine/threonine kinases, triggering phosphorylation of Smad1/5/8 in the cytoplasm. Phosphorylated Smad1/5/8 then forms a trimetric complex with Smad4 followed by translocation to nucleus, where they regulate the transcription of target genes for osteoblast differentiation. In particular, homeobox gene Dlx5, which is an

upstream target of both BMP-2/Smad dependent and BMP-2/Smad independent pathways, plays a pivotal role in stimulating the downstream transcription factors such as Runx2 and Osx [28]. MAPKs (including ERK, p38 and JNK) signaling, which are upstream regulators of Dlx5 in the BMP-2/Smad independent pathway, has been found to play important role in osteoblast differentiation, regulating the ALP, Runx2 and OCN expressions [28]. Interestingly, the involvement of BMP-2/Smad dependent pathway in SeNPs mediated osteoblast differentiation has been recently reported [80]. Thus, in this study, we investigated whether Cs4-SeNPs mediated osteoblastogenesis is related to BMP-2 signaling like other SeNPs using the MC3T3-E1 cells. A time-dependent study on the gene expression of major osteogenic markers (such as Dlx5, ALP, Runx2, Osx, OCN and OPG/RANKL) as well as protein expression and phosphorylation of BMP-2 and Smad1/5/8 triggered by the Cs4-SeNPs was performed in the MC3T3-E1 cells by qPCR and Western blotting, respectively. Besides, in order to determine the role of MAPKs signaling in the Cs4-SeNPs mediated osteoblast differentiation, a time-dependent study on the protein expression and phosphorylation of ERK, p38 and JNK triggered by the Cs4-SeNPs was also conducted in the MC3T3-E1 cells.

1.9.4 To study the cellular uptake behavior of Cs4-SeNPs

Endocytosis has been widely reported as the major cellular uptake mechanism for

nanoparticles [81]. In this study, the cellular uptake behavior of Cs4-SeNPs by the MC3T3-E1 cells was traced intracellularly by fluorescence microscopy as previous described.

We anticipate that findings of this study could provide significant insights into the *in vitro* effects of Cs4-SeNPs on osteoblastogenesis. Our long-term goal is to develop an evidence-based bone-forming agent for promoting the bone health of postmenopausal patients in our community.
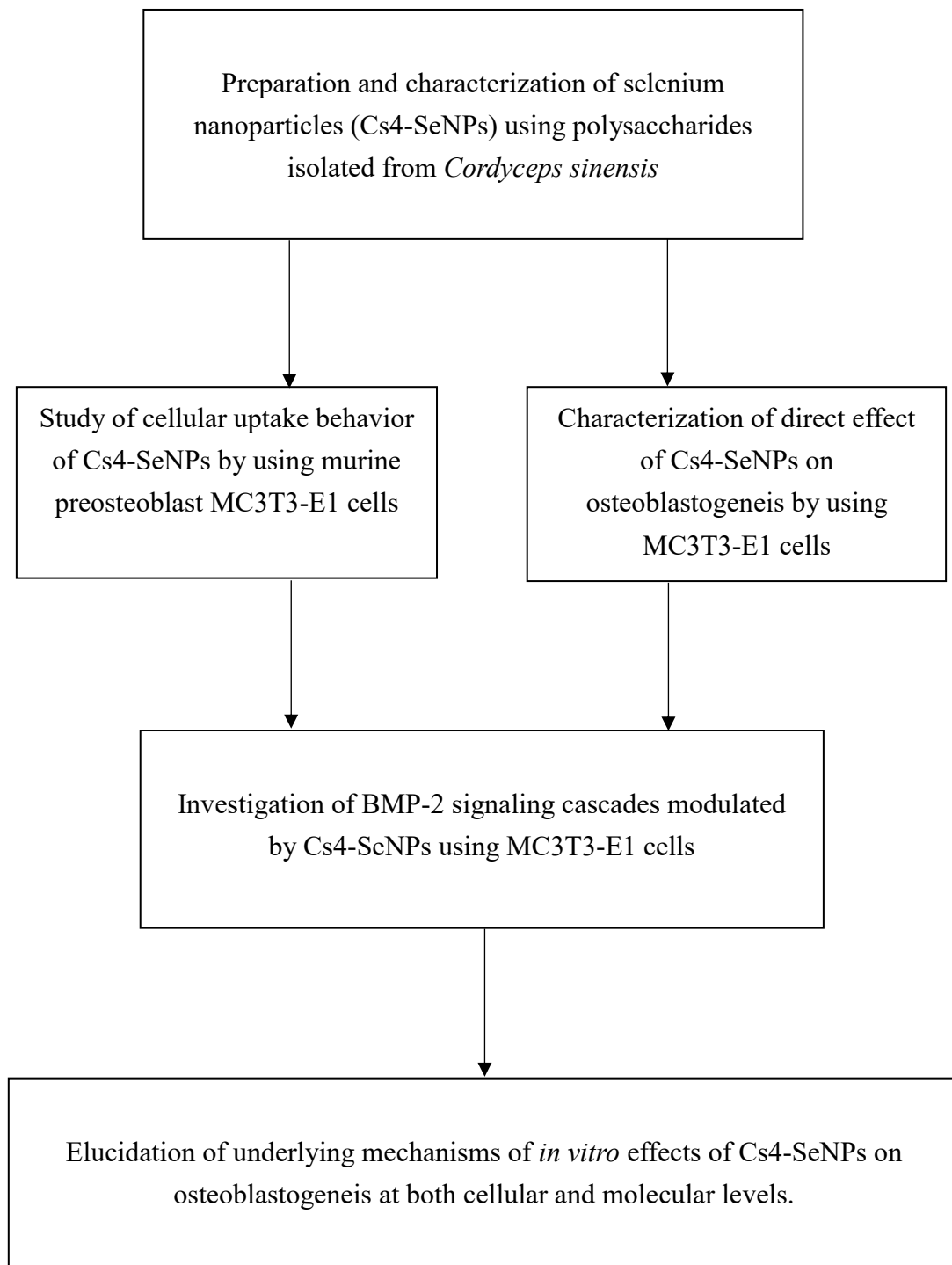
Figure 4. Project Summary

2   Materials and Methods

2.1 Chemicals and Reagents

All chemicals were analytical grade and purchased from Sigma-Aldrich Co. (St. Louis, MA, USA) unless specifically stated.

2.2 Hot Water Extraction of *Cordyceps sinensis* Polysaccharides

About 500g of *Cordyceps sinensis* mycelium powder (Cs4) purchased from Hong Kong Institute of Biotechnology (HKIB) was firstly undergone hot water extraction [1:20 (w/v); 95-100°C] for 2 hrs. After cooling, the hot water extract was centrifuged (18,600 × g; 1 hr; 4 °C) and the residue was further extracted under the same conditions. All supernatant collected was then pooled together and concentrated by using a rotary evaporator at 60°C followed by centrifugation (18,600 × g; 1 hr; 4°C). Subsequently, the concentrated supernatant was dialyzed with Spectra/Por® Dialysis Membrane (Mw cutoff: 8,000) until its total dissolved solute (TDS) was similar to that of Milli-Q water. The resulting dialysate (Cs4 polysaccharides) was then freeze-dried into powder by FreeZone 6L Console Freeze Dry Systems with Stoppering Tray Dryer (Labconno, USA) and stored in desiccator prior to further SeNPs preparation.

2.3 <u>Preparation of Cs4-SeNPs</u>

In brief, 4mL of aqueous Cs4 polysaccharides was firstly mixed with 25mM aqueous sodium selenite under magnetic stirring for 2 hrs. One milliliter of 100mM freshly prepared ascorbic acid was then added into the solution drop-wisely with stirring followed by reconstituting with ultrapure water to 10mL. After stirring under room temperature for 10 min, the solution was allowed to react for 24 hrs at 4°C before extensive dialysis (Mwcutoff: 8,000) until its TDS was similar to that of Milli-Q water. The resulting dialysate, Cs4-SeNPs was stored at 4°C prior to further composition analysis and structural characterization.

2.4 <u>Composition Analysis and Structural Characterization of Cs4-SeNPs</u>

2.4.1 Selenium concentration of Cs4-SeNPs

In brief, 10mL of trace metal grade 70% concentrated nitric acid was firstly added to 0.5mL of Cs4-SeNPs followed by microwave digestion using ETHOS One Advanced Microwave Digestion System (Milestone S.r.l., Italy). A temperature program with temperature rising from 180°C (holding for 20 min) to 250°C (holding for 30 min) was adopted. Digestate of Cs4-SeNPs was then diluted with Milli-Q water in a 25mL volumetric flask. After filtered with 0.45μm cellulose acetate syringe filter, Se

concentration in Cs4-SeNPs was determined by ICP-OES (Agilent 710, Agilent Technology Inc., USA) using 196.026 nm as emission wavelength and 203.985 nm as reference. For quantification, a standard curve of 0.1 ppm to 5 ppm selenium was prepared.

2.4.2 Particle size and stability of Cs4-SeNPs

To determine the particle size and stability of Cs4-SeNPs, Cs4-SeNPs was diluted 1,000 folds before injection into Nanosight NS3000 (Malvern Instrument Ltd., UK) using nanoparticles tracking analysis (NTA). For stability study, Cs4-SeNPs was stored at 4°C and its particle size was determined every two weeks for a total of 6 weeks.

2.4.3 Structural characterization of Cs4-SeNPs

In short, 30μL of Cs4-SeNPs was dropped onto a hollow carbon grid and allowed to air dry. The whole procedure was repeated for five times. The dried Cs4-SeNPs specimen was then visualized by JEM-2100F Field Emission Electron Microscope (JEOL Ltd., Japan) with 20,000×, 40,000× and 150,000× magnification using 200kV electron beam. One single nanoparticle was selected for further analysis of its elemental composition and crystallography under 150,000× magnification using HR-TEM-EDX (JEOL JEM-2100F + Horiba EX-250). All experimental results were analyzed by

software ImageJ.

2.4.4 Association between SeNPs and Cs4 polysaccharides

In brief, freeze-dried Cs4-SeNPs and Cs4 polysaccharides were individually milled with potassium bromide (KBr) under 57% relative humidity. The pellet discs of Cs4-SeNP-KBr mixture and Cs4 polysaccharides-KBr mixture were then prepared and their infrared spectra were obtained and compared by Nicolet^{TM} iS^{TM} 50 Fourier Transform Infrared Spectrometer (FT-IR). The major functional groups that are responsible for the association between Cs4 polysaccharides and SeNPs were determined accordingly.

2.5 Cell Culture

MC3T3-E1 subclone 4 preosteoblast cells (ATCC; CCRL-2593, Rockville, MD, USA) were maintained in ascorbic acid free alpha-minimum essential medium (α-MEM; Invitrogen, San Diego, CA, USA) supplement with 10% fetal bovine serum (FBS; Invitrogen, San Diego, CA, USA) as well as 1% 100× antibiotics and anti-mycotics (Invitrogen, San Diego, CA, USA). The cells were cultured in a 37ºC incubator with 95% relative humidity and 5% CO_2 and were routinely passaged by using 0.25% trypsin/0.1%EDTA at 80% confluence after 7 days.

2.6 Direct Effects of Cs4-SeNPs on Osteoblastogenesis

2.6.1 Cell proliferation

Cells pretreated with different concentrations of Cs4-SeNPs (0.1nM - 10µM), 6µg/mL of Cs4 polysaccharides, 10µM of sodium selenite or 10µM of selenomethionine were then incubated for 24, 48 and 72 hrs followed by determining cell proliferation using MTS [3-(4,5-dimethylthiazol-2-yl)-5-(3-carboxymethoxyphenyl)-2-(4-sulfophenyl)-2H-tetrazolium] assay (Promega). To perform MTS assay, 4.6 mg of phenazine methosulfate (PMS) was dissolved in 5 mL of PBS, while 42 mg of MTS powder was dissolved in 21 mL of PBS with pH adjustment to 6.0 – 6.5. Subsequently, 4.2 mL of MTS solution was mixed with 1 mL of PMS solution. After filtered with 0.22µM filter, cells were added into the MTS/PMS mixture in a ratio of 1:5 (20µL/well) and incubated for 1 hr at 37°C in a humidified incubator with 5% CO_2. Absorbance was determined at 490nm using a microplate reader (Clariostar, USA).

2.6.2 Cell differentiation, ALP activity and ALP staining

MC3T3-E1 cells are murine pre-osteoblasts which exhibit phenotypic differentiation from pre-osteoblast to osteoblast under induction of ascorbic acid. To

study osteoblastic differentiation, MC3T3-E1 cells (4.5×10^5 cells/well; 24-well plate)

cultured in osteogenic medium containing 10nM β-glycerophoshpate and 50 μg/mL

ascorbic acid were pretreated with different concentrations of Cs4-SeNPs (0.1nM -

10μM), 6μg/mL of Cs4 polysaccharides or 10μM of selenomethionine for 6 days. Fresh

culture media were replenished every 3 – 4 days.

To determine ALP activity, MC3T3-E1 cells were firstly washed with PBS

followed by lysed with 50mM Tris-HCl (200μL/well, pH 8.0) and 0.5% Triton X-100.

Cell lysates were then harvested and transferred into 1.5mL centrifuge tubes before

storage at -80°C. After defrosted, all lysates were centrifuged (12,000 × g; 2 min; 4°C)

and 10μL of supernatant was added into 96 wells in triplicate followed by incubation

with 200μL of 10mM p-nitrophenyl phosphate (pNPP) in 1M diethanolamine and

0.5mM MgCl$_2$ (pH 9.8) for 15 – 30 min. Consequently, the reaction was quenched by

adding 50μL of 3M NaOH and the resulting absorbance was measured at 405nm using

a microplate reader (Clariostar, USA). To normalize the ALP activity, the total protein

content was also determined by bicinchoninic acid (BCA) assay. In short, 200μL of

BCA solution (Thermo, USA, mixing BCA reagent A with B at a ratio 98:2) was added

into a well containing 2μL of protein sample and 23μL of water followed by incubation

at 37°C for 30 min. Similarly, the resulting absorbance was measured at 595nm using a

microplate reader. Besides, ALP-containing cells (osteoblasts) were visualized by using an alkaline phosphatase kit (Sigma-Aldrich) according to the manufacturer's instructions. In brief, MC3T3-E1 cells (9×10^4 cells/well; 6- well plate) pretreated with 10µM of Cs4-SeNPs for 6 days were washed with PBS and fixed with 10% formalin for 15 min. The ALP in cells were then stained by Fast Blue RR salt and Naphthol AS-MX phosphate alkaline solution for 60 min followed by rinsing thoroughly with deionized water. They were dried by air and the results were visualized.

2.6.3 Mineralization assay, Von Kossa and Alizarin Red S staining

To study bone mineral formation, MC3T3-E1 cells (4.5×10^5 cells/well; 6- well plate) cultured in osteogenic medium containing 10nM β-glycerophoshpate and 50µg/mL ascorbic acid were pretreated with 10µM of Cs4-SeNPs, 6mg/mL of Cs4 polysaccharides, or 10µM of selenomethionine for 18 days. The medium was replenished for every 3 - 4 days. Bone nodules formed in the MC3T3-E1 cells were then visualized and compared by Von Kossa and Alizarin Red S staining.

To detect phosphate deposit by Von Kossa staining, cells were pre-washed with PBS and fixed with 10% formalin for 15 min. Fixed cells were then treated with 5% silver nitrate for 30 min under light following by sequential washing with deionized

water, 5% sodium carbonate in 10% formalin (1 min), deionized water and 5% sodium thiosulfate (5 min). Consequently, stained well was captured and analyzed by ImageJ to semi-quantify phosphate deposition.

For Alizarin Red S staining, similarly, cells were pre-washed with PBS and fixed with 10% formalin for 15 min. Fixed cells were then stained with 1 ml of 40mM Alizarin Red S solution (pH 4.1) for 20 min with gently shaking followed by heavy washing 4 times with 4 mL of deionized water for 5 min per well. Excessive water in the wells was removed and the resulting image was captured. To quantify the calcium deposit, 800µL of 10% (v/v) glacial acetic acid was added into each well followed by incubation with shaking for further 30 min. All stained cells were then scraped with cell scraper and transferred into a 1.5mL centrifuge tube using acetic acid. After vortex-mixing for 30 s, 500µL of mineral oil was added and the slurry was heated up to 85°C for 10 min followed by cooling down in ice for 5 min. All tubes were then centrifuged at 20,000 × g for 15 min and 500µL of the supernatant was transferred into new Eppendorf tubes. After adding 200µL of 10% (v/v) ammonium hydroxide, the mixture was aliquot in a 96 well plate in triplicate followed by measuring the absorbance with a microplate reader at 405nm.

2.6.4 Total RNA isolation and real-time polymerase chain reaction (qPCR)

To further characterize the direct effects of Cs4-SeNPs on osteoblastogenesis, mRNA expression of major osteogenic markers (such as ALP, Dlx5, Runx2, Osx, OCN and OPG/RANKL) in the MC3T3-E1 cells (4.5×10^5 cells/well; 6 well plate) pretreated with 10µM of Cs4-SeNPs for 6 and 9 days were quantified by real-time PCR. For total RNA extraction, cells were washed twice with 1 mL of ice cold PBS and total RNA was isolated with 1mL of Trizol reagent per 6 wells according to manufacturer's protocol (Life technologies, USA). After homogenization, 200µL of chloroform was added with gentle shaking and the mixture was allowed to stand for 3 min at room temperature. All samples were then centrifuged ($12,000 \times g$; 10 min; 4ºC) and the top aqueous layers were transferred into new tubes prior to adding 500 µL of 2-propanol. Subsequently, the whole reaction mixture was centrifuged under the same conditions and the 2-propanol was removed followed by washing with 1mL of 75% ethanol in DEPC H_2O. After centrifugation ($7,500 \times g$; 5 min; 4ºC), the 75% ethanol was removed and the RNA pellet was air-dried. Once the RNA pellets turned into milky, 10 - 20µL of DEPC H_2O was added to re-dissolve the RNA and stored at -80ºC.

For qPCR analysis, 20ng of RNA was firstly prepared by One-Step RT-qPCR kit (TAKARA) according to manufacturer's instructions. In a 20µL reaction, the reaction

mixture contained 10µL of 2X One Step RT-PCR Buffer, 0.8µL of PrimeScript One-Step Enzyme Mix 2, 0.4µM of Forward PCR primers, 0.4µM of Reverse PCR primers and 20ng of RNA sample. qPCR analysis of major osteogenic markers (such as ALP, DLx5, Runx2, Osx, OCN and OPG/RANKL) was performed by a Pikoreal thermal cycler system (Thermo, USA) using thermal cycling program and primers shown in **Table 1** and Table 2, respectively. Relative mRNA expression of each osteogenic marker gene was normalized to that of GAPDH, which is a common housekeeping gene.

Table 1. Thermal cycling program for qPCR analysis

Stage	Temperature	Hold Time
Reverse Transcription (1 cycle)	42°C	5 min
	95°C	10 sec
PCR reaction (40 cycles)	95°C	5 sec
	60°C	20 sec
Melting Curve Analysis	95°C	0 sec
	65°C	15 sec
	95°C	0 sec

Table 2. Primer list for qPCR analysis

Gene	Forward Primer (5'-3')	Reverse Primer (5'-3')
Runx2	AAGTGCGGTGCAAACTTTTCT	TCTCGGTGGCTGGTAGTGA
Dlx5	GTTTCAGAAGACTCAGTACCT	TGACTGTGGCGAGTTACAC
ALP	AACCCAGACACAAGCATTCC	GAGAGCGAAGGGTCAGTCAG
Osx	AGAGGTTCACTCGCTCTGACGA	TTGCTCAAGTGGTCGCTTCTG
OPG	ACGAACTGCAGCACATTTGG	TGTTTCCGGAACACACGTTG
RANKL	ACGCCAACATTTGCTTTCGC	ATTGCCCGACCAGTTTTTCG
OCN	TAGTGAACAGACTCCGGCGCTA	TGTAGGCGGTCTTCAAGCCAT
GAPDH	CATGGCCTTCCGTGTTCCTA	CCTGCTTCACCACCTTCTTGAT

2.6.5 Total protein extraction and western blot analysis

With a purpose to dissect the BMP-2 signaling (both Smad dependent and independent pathways) mediated by Cs4-SeNPs during osteoblast differentiation, protein expression and phosphorylation of BMP-2, Smad1/5/8 ERK, p38 and JNK in the MC3T3-E1 cells (4.5×10^5 cells/well; 6 well plate) pretreated with 10μM of Cs4-SeNPs for 3 days were determined by Western blot analysis. For total protein extraction, cells were washed twice with PBS and lysed with 50μL of RIPA Lysis buffer containing PMSF and 1X protease and phosphatase inhibitor cocktail. Cells were then scraped and transferred into 1.5mL centrifuge tubes followed by sonication (1 min) and centrifugation ($22,000 \times$ g; 20 min; 4°C). Total protein content of the supernatant was

determined by BCA protein assay at 562nm. After mixed with 4X sample buffer, the reaction mixture was heated up to 95°C for 5 min and stored at -20°C.

For Western blotting, 40μg of protein sample was loaded and separated by 10% SDS-PAGE using gel electrophoresis. Separated proteins were then transferred to PVDF membranes using iBlot 2 Dry Blotting System. After blocking with 5% BSA (w/v) or 5% blocking grade non-fat dry milk powder (Bio-rad, USA) in Tris-buffered saline containing 0.1% (v/v) Tween-20 (TBST) for 1 hr at room temperature, all membranes were incubated with specific primary antibodies including BMP-2, p-Smad 1/5/8, Smad 1/5/8, p-ERK, ERK, p-p38, p-38, p-JNK, JNK and GAPDH [dilution: 1:1000; 5% BSA in TBST] at 4°C overnight. Subsequently, all membranes were extensively washed with TBST and incubated with the secondary anti-mouse IgG HRP-linked antibodies at 1:2000 dilution for 1 hr at room temperature. Finally, the membranes were further washed with TBST, while chemiluminescence for detection was developed using EMD Millipore Immobilon Western Chemiluminescent HRP substrate (Millipore, USA) according to the manufacturer's instructions. Image acquisition was performed using Azure™ c600 digital imager (Azure Biosystem Inc., USA) followed by quantification with ImageJ.

2.6.6 Cellular uptake behavior of Cs4-SeNPs

In brief, MC3T3-E1 cells were firstly seeded in a 35mm confocal dish for 24 hrs followed by sequential staining with Hochest 33342 (1µg/mL; nucleus; Invitrogen, CA, USA) and Lysotracker Deep Red (25µM; lysosomes; Invitrogen, CA, USA) for 20 and 30min, respectively. After further incubation with 10µM of coumarin-6-loaded Cs4-SeNPs at 37°C for 10 min, the cellular uptake behavior of Cs4-SeNPs by MC3T3-E1 cells was intracellularly traced by fluorescence microscopy (Zess Lightsheet Z.1 Microscope).

2.7 Statistical Analysis

All experiments were conducted in triplicates and results were presented as mean ± SEM. Except gene expression and mineralization results, which were analyzed by two-tailed Student's *t*-test, all mean values were analyzed by parametric one-way ANOVA followed by multiple comparisons using Turkey-HSD to detect significant differences at $p < 0.05$, $p < 0.01$ $p < 0.001$ (GraphPad Prism, San Diego, CA, USA).

3.   Results and Discussion

3.1 Preparation and Characterization of Cs4-SeNPs

Based on our patented nanotechnology (US patent no.: 9,072,669), novel Cs4-Se nanocomposites (Cs4-SeNPs) have been successfully prepared followed by characterization using Nanosight NS300, TEM (Hitachi H-7650), HR-TEM-EDX (JEOL-2010 + Horiba EX-250) and FT-IR (Equinox 55, Bruker). Nanoparticle tracking analysis (NTA) measures particle size using laser to track the movement of nanoparticles within a period of time, calculating their particles size according to the rate of Brownian motion and Stokes-Einstein equation. Based on the NTA using Nanosight NS300, size distribution of the Cs4-Se nanocomposite was found to has a mode of 66nm (**Figure 5A**) with an average particle size of 73.2 ± 3.49nm. As shown in **Figure 5B**, the average particle size of Cs4-Se nanocomposite was highly stable without significant change in size (± 10nm) after 6 weeks' storage at 4°C, suggesting its relatively high stability compared to other SeNPs prepared by using bovine serum albumin [68].

For HR-TEM, images are produced by differential amount of electron beam passing through the specimen and background, creating a darker areas for more electron dense regions [82]. In this study, further characterization of Cs4-SeNPs using HR-TEM (JEOL JEM-2100F; 200kV; magnification 40000×) also indicated that SeNPs itself (without mushroom polysaccharides decoration) existed as well-dispensed spherical particles in water with an average diameter of around 30nm (**Figure 5C**). At present, the most widely accepted definition of "nanoparticles" is that at least two dimensions of the particle are less than 100nm in size [83]. For NTA, the particles size is determined by tracking the x and y axis Brownian motion of particles, involving 2 dimension calculation of hydrodynamic diameter [84]. For ImageJ analysis of HR-TEM image, the Feret diameter measured is the longest distance of 2 parallel planes of an object with any shape [85]. In the present study, as the average particle size of Cs4-SeNPs determined by both NTA and HR-TEM are less than < 100nm (**Figure 5**), Cs4-SeNPs met the international standards and could be regarded as "nanoparticles".

A

Average particle size: 73.2 ± 3.49

B

C

50 nm
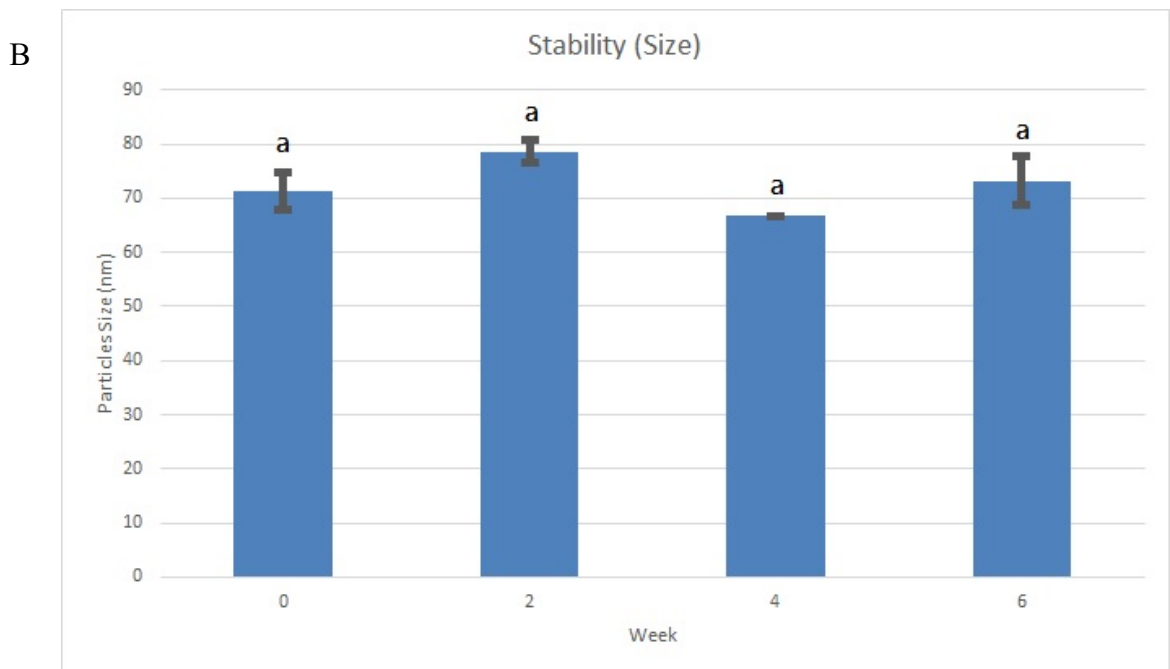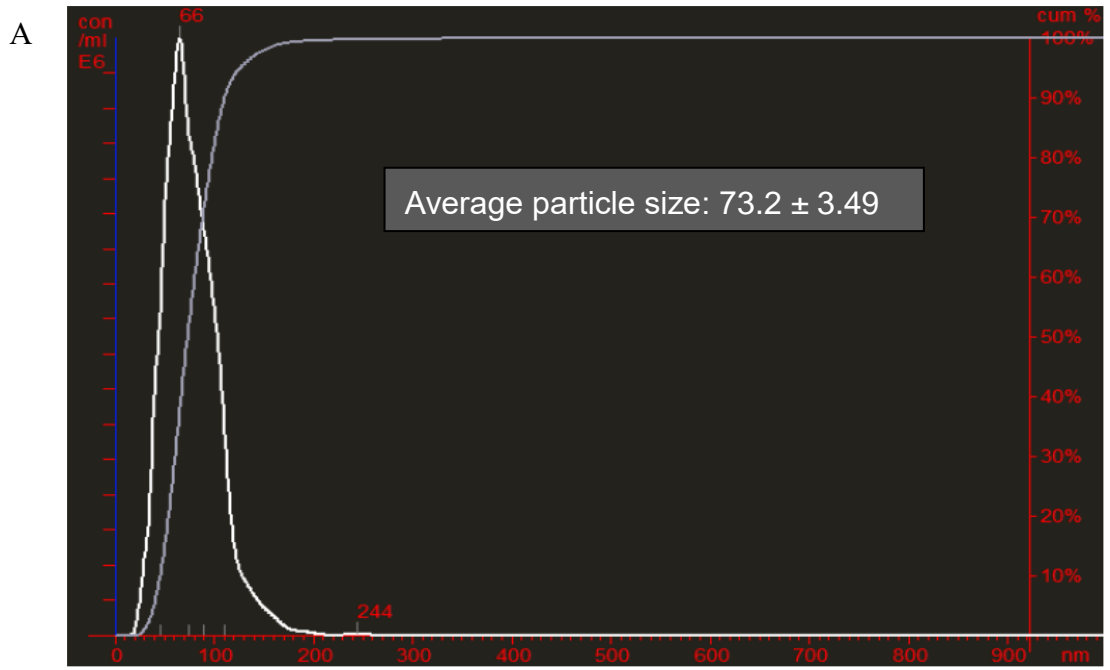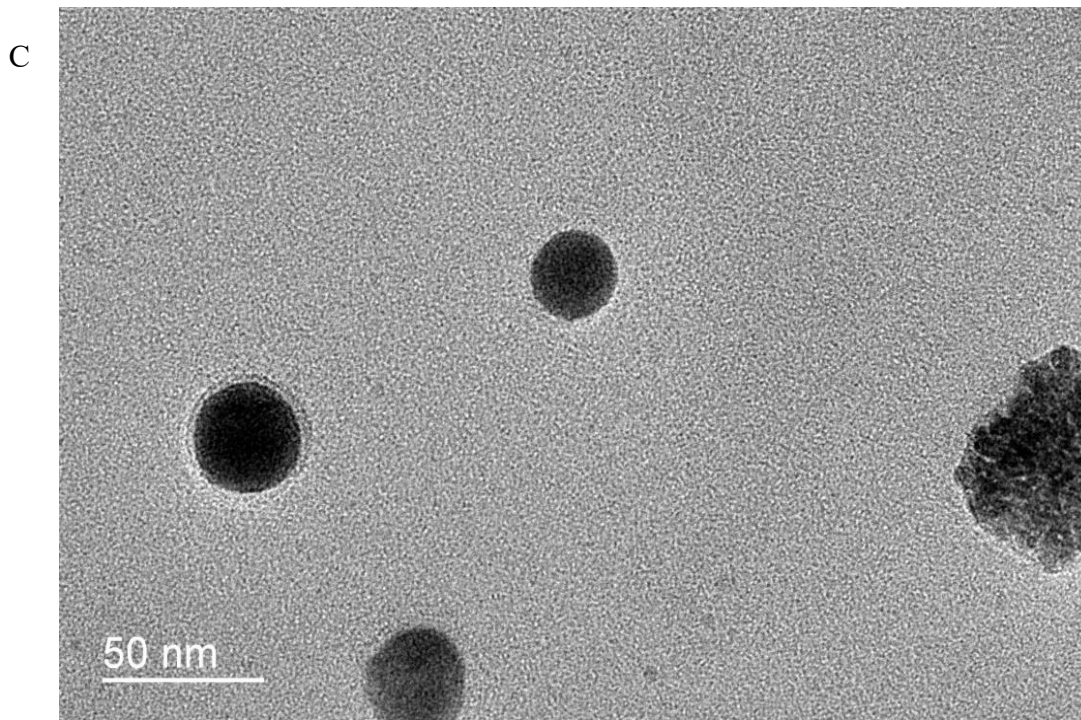
Figure 5. Particle size and stability of Cs4-SeNPs

(A) Particles size distribution of Cs4-SeNPs measured by Nanosight NS300. Cs4-SeNPs were diluted and its particle size distribution was determined by nanoparticle tracking analysis. (B) Time dependent study on stability of Cs4-SeNPs. Cs4-SeNPs were prepared and stored at 4°C for 6 weeks. Samples of Cs4-SeNPs were collected every 2 weeks and their particles size was measured by Nanosight NS300. Particle size was measured 5 times for each independent determination and results were presented as mean value of three independent measurements ± S.D. (C) Representative TEM image of Cs4-SeNPs. Cs4-SeNPs were seeded on a hollow carbon grid and examined under HR-TEM (JEOL JEM-2100F; 200kV; magnification 40,000×; scale bar: 50nm).

In general, there are three different kinds of crystalline structure including monocrystalline, amorphous crystal and polycrystalline. Selected area electron diffraction (SAED) is a widely used microscopy technique to determine the atom arrangement of crystalline by HR-TEM. For individual Cs4-SeNP, in addition to having clear lattice fringes/d-spacing (3.35Å; **Figure 6A**), the SAED pattern of Cs4-SeNPs exhibited a series of concentric rings constructed with white dots (**Figure 6B**), collectively indicating that the nanoparticle possessed a polycrystalline structure [82].

HR-TEM-EDX is another microscopy technique for determining the elemental composition by HR-TEM. Each element has unique energy pattern for its own electron shells. When the electron beam of HR-TEM kick out the electron from ground state, the electron with higher energy state from outer electron shell will then fill the vacancy of inner electron shell and release energy in form of X-ray. Thus, different elements can be identified and quantified due to the specific energy difference between their corresponding electron shells. **Figure 6C** showed that Cs4-SeNPs contained very high level of Se (83.9%), indicating a successfully fabrication of SeNPs using mushroom polysaccharides. Some minor peaks may be due to the present of copper originated from the carbon film coated copper grid during HR-TEM-EDX sample preparation. Besides the results for carbon was eliminated as it would overestimate the percentage of carbon

in polysaccharides with the present of carbon atom on carbon film coated copper grid

In this study, the chemical binding of mushroom polysaccharides to the surface of SeNPs was further investigated by FT-IR spectrometry. As shown in **Figure 6D**, the two major absorption peaks at 1633.09 and 3000 – 4000cm^{-1} in the IR spectrum of Cs4 polysaccharides corresponded to the stretching vibrations of carbonyl groups (–C=O–) of its proteins and hydroxyl groups (–OH–) of its polysaccharides, respectively. Interestingly, Cs4 polysaccharides shared very a similar FT-IR spectrum to that of Cs4-SeNPs, indicating that Cs4 polysaccharides formed part of the Cs4-SeNPs nanocomposite. Nevertheless, both absorption peaks of carbonyl and hydroxyl groups and shifted from 3415.61 to 3416.27 and from 1633.09 to 1635.89, respectively, indicating the occurrence of interaction between the carbonyl and hydroxyl groups of Cs4 polysaccharides as well as the Se atoms as previously reported [86]. These results suggest that the SeNPs were capped by mushroom polysaccharides mainly through the formation of Se-O bonds, leading to a stable spherical structure of SeNPs.

A

3.35Å

10 nm

B

Diameter = 5.74 1/nm
Radius = 2.87 1/nm
d-spacing = 0.348nm

Diameter = 9.88 1/nm
Radius - 4.94 1/nm
d-spacing = 0.202nm

5 1/nm
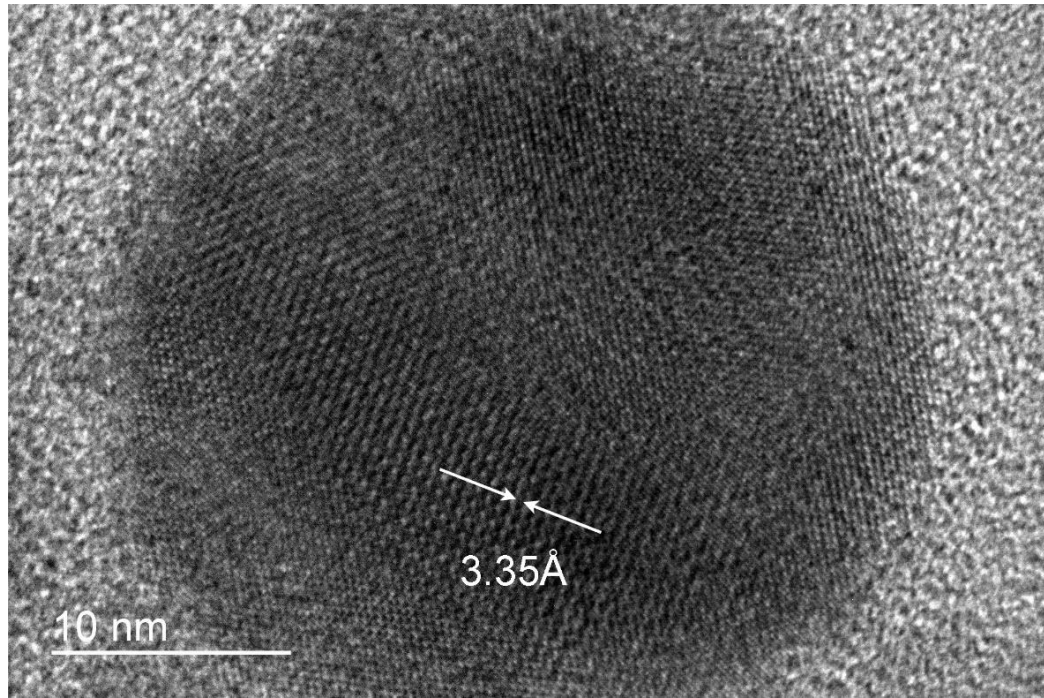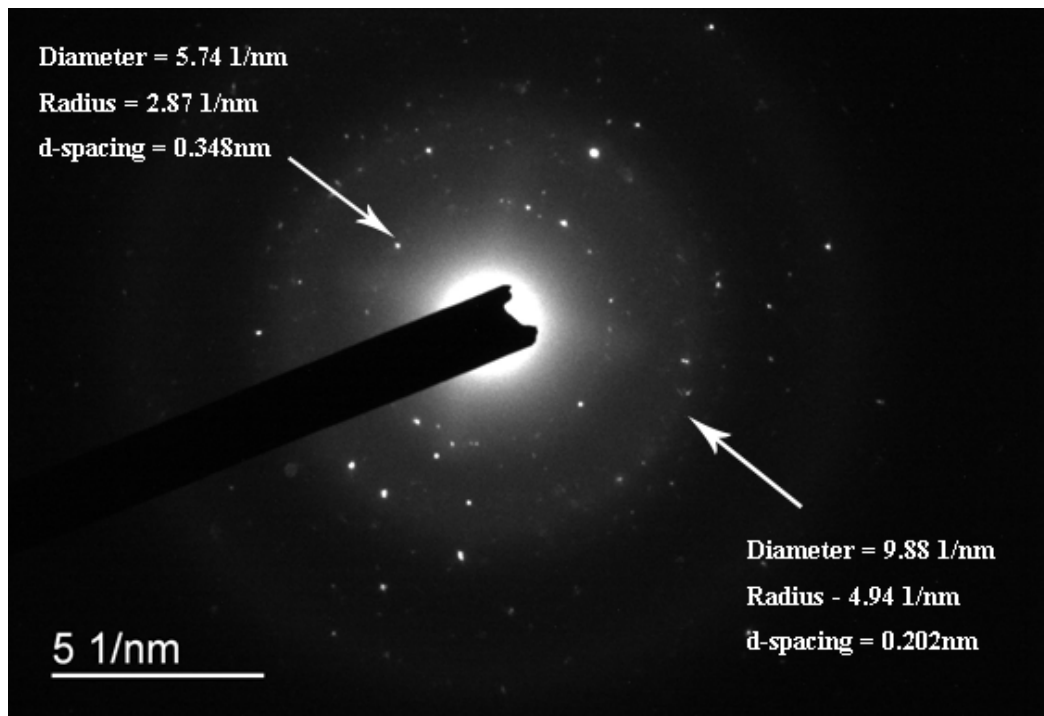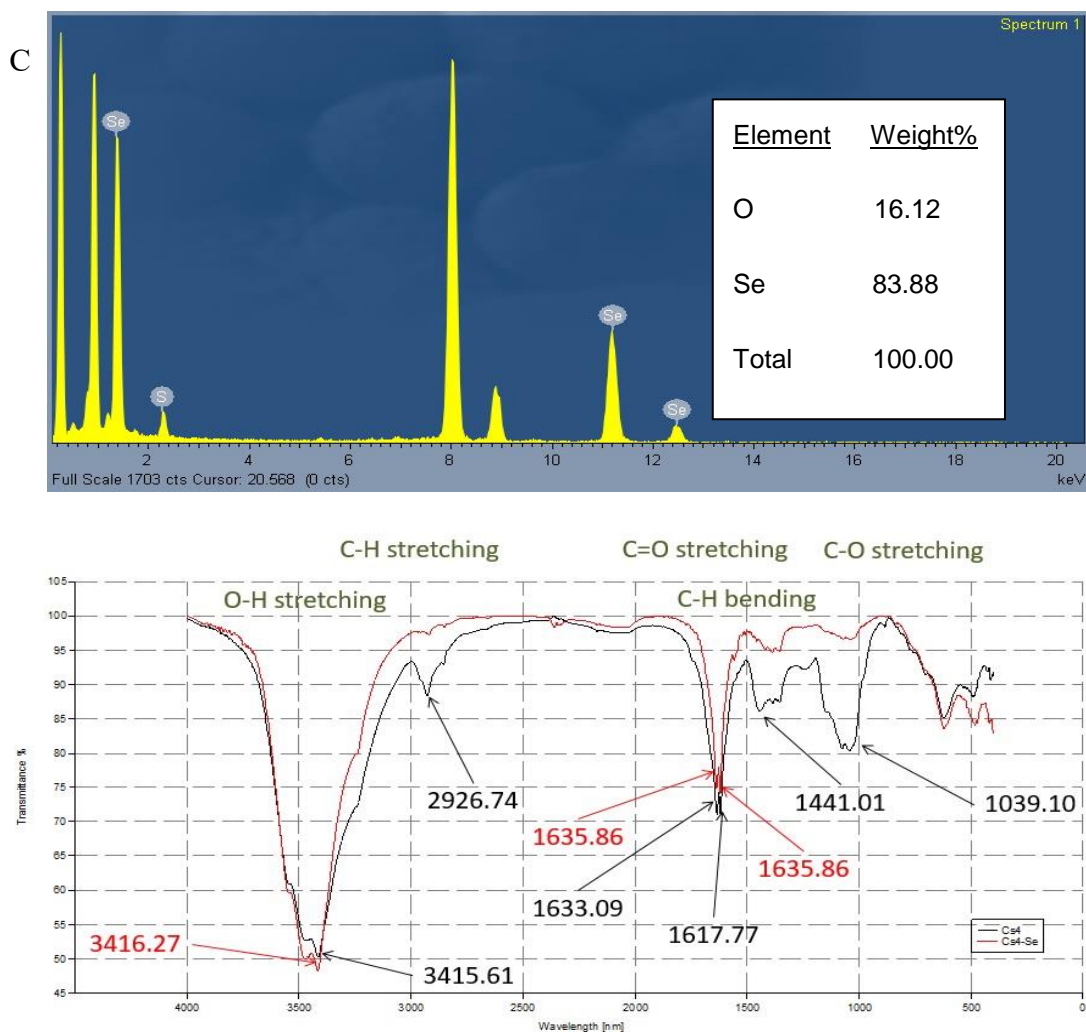
Figure 6. Elemental composition, crystallographic and fourier-transform infrared analysis of Cs4-SeNPs

Representative HR-TEM image of (A) lattice fringes and (B) corresponding selected area electron diffraction (SAED) pattern of Cs4-SeNPs. Cs4-SeNPs was seeded on a hollow carbon grid and examined under HR-TEM (20keV; 150000×). Lattice fringes as well as diameter, radius and d-spacing of diffraction rings were measured using ImageJ. (C) Representative EDX analysis of Cs4-SeNPs. (D) FT-IR analysis of Cs4-SeNPs and Cs4 polysaccharides. Freeze-dried Cs4-SeNPs and Cs4 polysaccharides were mixed with KBr to form sample discs followed by analysis using Nicolet™ iS™ 50 FT-IR Spectrometer.

3.2 <u>Direct Effects of Cs4-SeNPs on Osteoblastogenesis Using MC3T3-E1 Cells</u>

3.2.1 Cell Proliferation:

MTS assay is a widely used method to determine the proliferation of viable cells quantitatively by assuming that the MTS dye reduction is proportional to the number of viable cells in exponential growth. In short, PMS, acting as an intermediate electron acceptor, will penetrate the viable cells to transfer electron from cytoplasmic NADH, reducing tetrazolium salt (MTS) into soluble brightly colored formazan products [87-88].

In general, Cs4-SeNPs was found to exhibit a significant dose-dependent proliferation effect (range from 1.35 – 1.45 folds) on the MC3T3-E1 cells for 24, 48 and 72 hrs with the most effect dosage of 10μM (**Figure 7A-C**). A slightly drop of proliferation effect of Cs4-SeNPs from 24 to 72 hrs treatment might suggest an onset of cell differentiation at early stage of osteoblastogenesis, inhibiting cell proliferation [28]. In addition to sodium selenite (10μM; inorganic Se from common food source) and selenomethionine (10μM; organic Se from common food source), we further compared the proliferation effect of Cs4-SeNPs (10μM) and Cs4 polysaccharides alone at concentration used for preparing 10μM of Cs4-SeNPs (i.e. 6μg/mL) in order to investigate whether mushroom polysaccharides decoration would contribute the

proliferation effect of Cs4-SeNPs on MC3T3-E1 cells. Interestingly, both selenomethionine (10μM) and Cs4 polysaccharides had no effect on the proliferation of MC3T3-E1 cells, while sodium selenite (10μM) was found to significantly inhibit the growth of MC3T3-E1 cells for all time intervals (**Figure 8A-C**). In contrast, the significantly highest proliferation effect of Cs4-SeNPs on the MC3T3-E1 cells (**Figure 8A-C**) suggested that SeNPs itself, instead of polysaccharides, was mainly responsible for the proliferation effect of whole Cs4-Se nanocomposite, having relatively lower toxicity than that of sodium selenite under the same dosage. Since 10μM of sodium selenite exhibiting inhibiting effect on MC3T3-E1 cells, it was not involved in all experiments of further study on osteoblastogenesis. Besides, it is worth noting that, compared with the effective dosage (640μM) of other SeNPs on bone cell proliferation [89], Cs4-SeNP exhibited strong proliferation effect on bone cells with remarkable low concentration (10μM only).
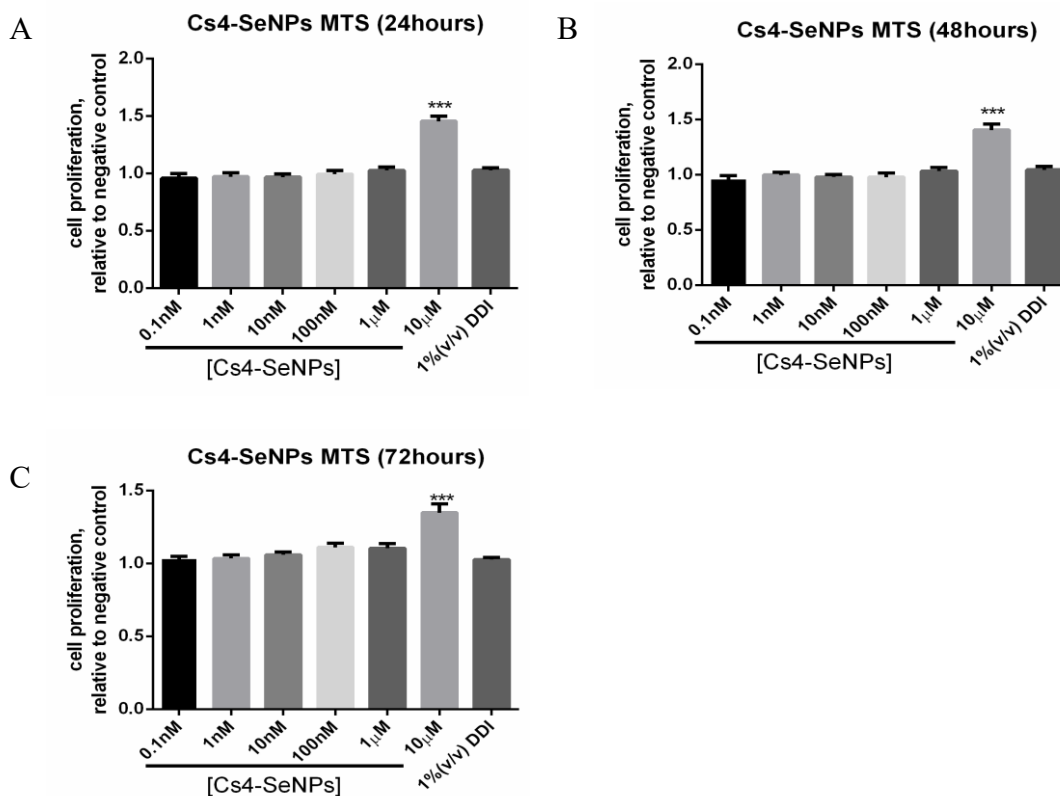
Figure 7. Dose and time-dependent study of the proliferation effect of Cs4-SeNPs on MC3T3-E1 cells.

Cells were treated with different concentrations of Cs4-SeNPs (0.1nM - 10μM) in normal medium for (A) 24 (B) 48 and (C) 72 hours. Cell proliferation was determined by MTS assay and results were normalized and compared with that of negative control group (1% deionized water; 1% DDI). Results are mean values of three determinations ± SEM. Means with "***" are significantly different ($p < 0.001$, one-way ANOVA).
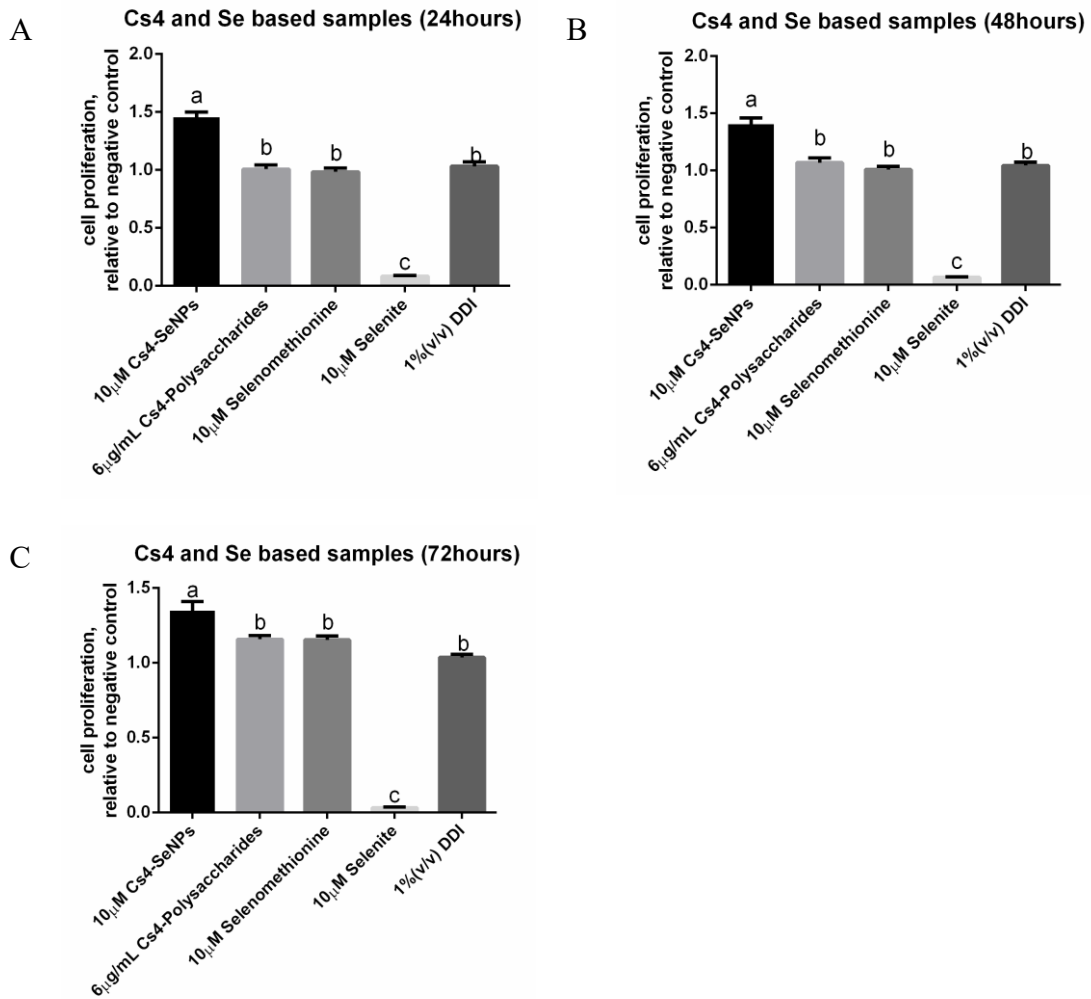
Figure 8. Comparative study of proliferation effect of Cs4-SeNPs, Cs4 polysaccharides, selenomethionine (SeMet) and sodium selenite on MC3T3-E1 cells.

Cells were treated with Cs4-SeNPs (10μM), Cs4 polysaccharides (6μg/mL), SeMet (10μM) and sodium selenite (10μM) in normal medium for (A) 24, (B) 48 and (C) 72 hours. Cell proliferation was determined by MTS assay and results were normalized and compared with negative control group (1% deionized water; 1% DDI). Results are mean values of three determinations ± SEM. Means with letters (a-c) are significantly different ($p < 0.05$, one-way ANOVA).

3.2.2 Osteoblastic differentiation and bone mineralization formation

Alkaline phosphatase (ALP) is a phosphor-hydrolytic enzyme that plays a major role in osteoblastogenesis, regarding as a phenotypic marker for osteoblasts during differentiation and mineralization. As shown in **Figure 9A & Figure** 11**C**, Cs4-SeNPs (10μM) markedly induced the osteoblastic differentiation of MC3T3-E1 cells after a 6-day treatment as evidenced by a significant increase in ALP activity (3.05 ± 0.15 folds) and up-regulation of ALP gene expression (1.77 folds). In contrast, both SeMet (10μM) and Cs4 polysaccharides (6μg/mL) did not exhibit any effect on the ALP activity. The ALP containing MC3T3-E1 cells pre-treated with 10μM of Cs4-SeNPs (purple-blue area) were further visualized by ALP staining (**Figure 9C**).

Mineralization is the final stage of osteogenesis and hydroxyapatite $[Ca_{10}(PO_4)_6(OH)_2]$ is the major component of bone, consisting of calcium and phosphate. In bone research, Alizarin Red S and Von Kossa staining are the two widely used staining methods targeting the calcium and phosphate in hydroxyapatite, respectively. In short, Alizarin Red S staining visualizes the calcium in hydroxyapatite (red dots) by interacting the calcium ions with sulfonic acid or -OH groups of Alizarin Red S. For Von Kossa staining, the phosphate in hydroxyapatite is visualized (black dots) by reacting the silver ions with phosphate under illumination, forming silver

phosphate. As shown in **Figure 10A-C**, unlike SeMet (10μM) and Cs4 polysaccharides (6μg/mL), Cs4-SeNPs (10μM) significantly promoted the bone nodule formation in MC3T3-E1 cells after 18-day treatment as visualized by both Von Kossa and Alizarin Red S staining as well as the semi-quantification of calcium deposition by imageJ (Alizarin Red S staining: 1.45 ± 0.12 folds). Osteocalcin (OCN), which expresses in differentiating cells of intermediate and mature nodules, is a specific marker gene for mineralization. Further investigation on the gene expression of OCN also indicated that Cs4-SeNPs (10μM) could significantly up-regulate this mineralization maker gene for 2.64 ± 0.14 folds (**Figure 11E**), demonstrating its strong stimulating effect on bone mineralization.

Runx2 and osterix (Osx) are the two main osteoblastic transcription factors in osteogenesis [90-91]. Runx2 highly expresses in early differentiation stage in calcified cartilage and bone tissues to induce osteoblastogenesis by regulating bone matrix protein and inhibiting cell proliferation. Activation of Runx2 has also been found to upregulate several osteoblast-specific genes (such as OCN), promoting bone formation in both cell and animal models [92-94]. Similarly, Osx is another critical transcriptional factor in osteoblast differentiation and bone formation previously identified in a Osx-null mutant mice study [50]. As shown in **Figure 11A & D**, the gene expression of both

Runx2 (1.48 ± 0.06) and Osx (1.46 ± 0.08) in MC3T3-E1 cells pre-treated with 10μM of Cs4-SeNPs for 6 days were significantly up-regulated, indicating that Cs4-SeNPs (10μM) enhanced the osteoblastic differentiation and bone formation in MC3T3-E1 cells mediated by these two transcription factors.

Bone remodeling is a lifelong process of regulating "new bone formation" and "old bone resorption". These two sub-processes are governed by specialized cell types named "osteoblast" as well as "osteoclast" and an imbalance of which results in metabolic bone diseases like osteoporosis [26]. Osteoprotegerin (OPG) and receptor activator of NFkB ligand (RANKL) are bone remodeling markers secreted by osteoblasts for inhibiting or activating osteoclasts, respectively [95-96]. RANKL triggers osteoclast differentiation by binding with RANK, while OPG acts as a competitor to block the RANKL/RANK interaction to limit osteoclast differentiation[97]. Thus, OPG/RANKL ratio is a widely used parameter to figure out the possible interaction between osteoblasts and osteoclasts. Interestingly, our study discovered that Cs4-SeNPs (10μM) significantly up-regulate the expression of both OPG and RANKL to different extent, resulting in significant increase of the OPG/RANKL ratio (2.56 ± 0.24 folds; **Figure 11F**). In addition to direct promoting osteoblastogenesis, this finding suggested that Cs4-SeNPs (10μM) also exhibited indirect inhibition effect on osteoclastogenesis.
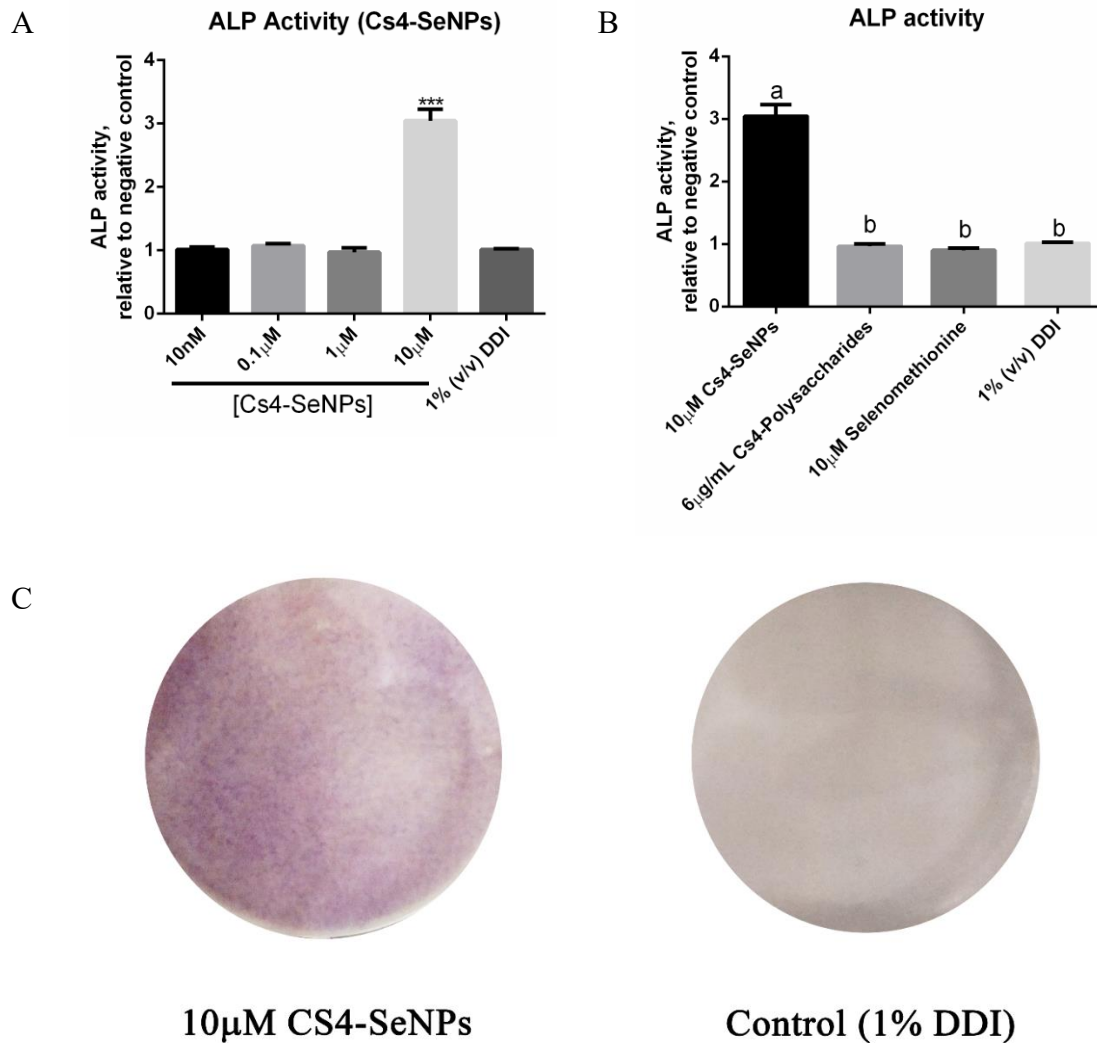
Figure 9. Cs4-SeNPs induced osteoblastic differentiation in MC3T3-E1 cells.

(A) ALP activity in MC3T3 cells pre-treated with different concentrations of Cs4-SeNPs (10nM-10μM) and (B) Cs4-SeNPs (10μM), Cs4 polysaccharides (6μg/mL) or SeMet (10μM) in osteogenic medium for 6 days was determined by spectrophotometry at 405nm and normalized relative to the total cellular protein content. Normalized results were compared with that of the negative control group (1% deionized water; 1%DDI). (C) ALP containing MC3T3-E1 cells pre-treated with 10μM of Cs4-SeNPs or 1% (v/v) DDI were visualized by ALP staining. Results are mean values of three determinations ± SEM. Means with "***" and letters (a-b) are significantly different at $p < 0.001$ and $p < 0.05$, respectively (one-way ANOVA).

A

10μM CS4-SeNPs   6μg/mL CS4-Polysaccharide   10μM Selenomethionine   Control (1% DDI)

B

10μM CS4-SeNPs   6μg/mL CS4-Polysaccharide   10μM Selenomethionine   Control (1% DDI)

C   **Semi Quantitation of Alizarin Red Staining**
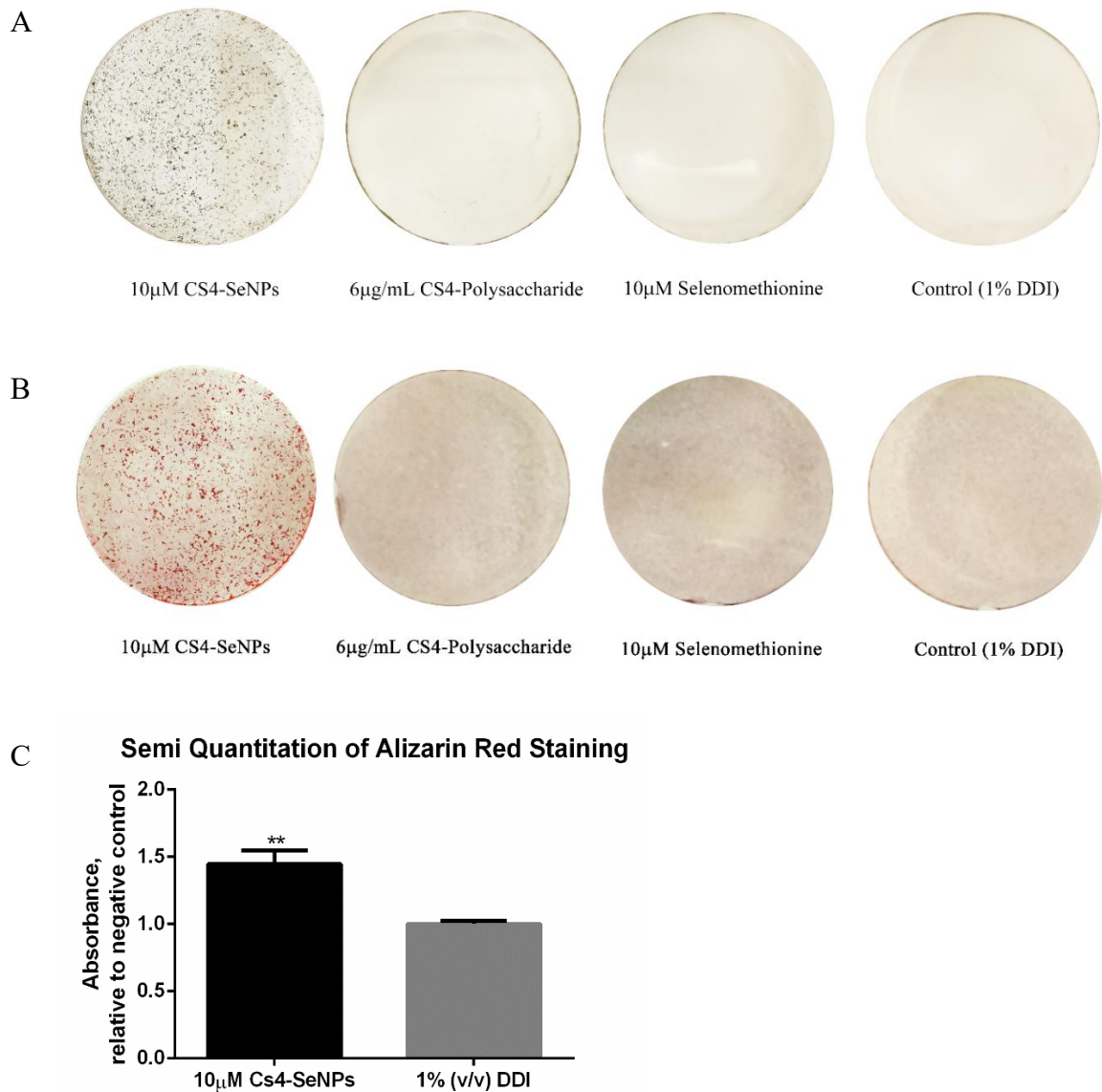
Figure 10. Cs4-SeNPs simulated bone mineral formation in MC3T3-E1 cells.

Bone nodules formation in MC3T3-E1 cells pre-treated with Cs4-SeNPs (10μM), Cs4 polysaccharides (6μg/mL) or SeMet (10μM) in osteogenic medium for 18 days was visualized by (A) Von Kossa staining and (B) Alizarin Red S staining. (C) Semi-quantification of Alizarin Red S staining was determined by spectrophotometry. Results are mean values of three determinations ± SEM. Means with "**" are significantly different ($p < 0.01$; Student's t-test).
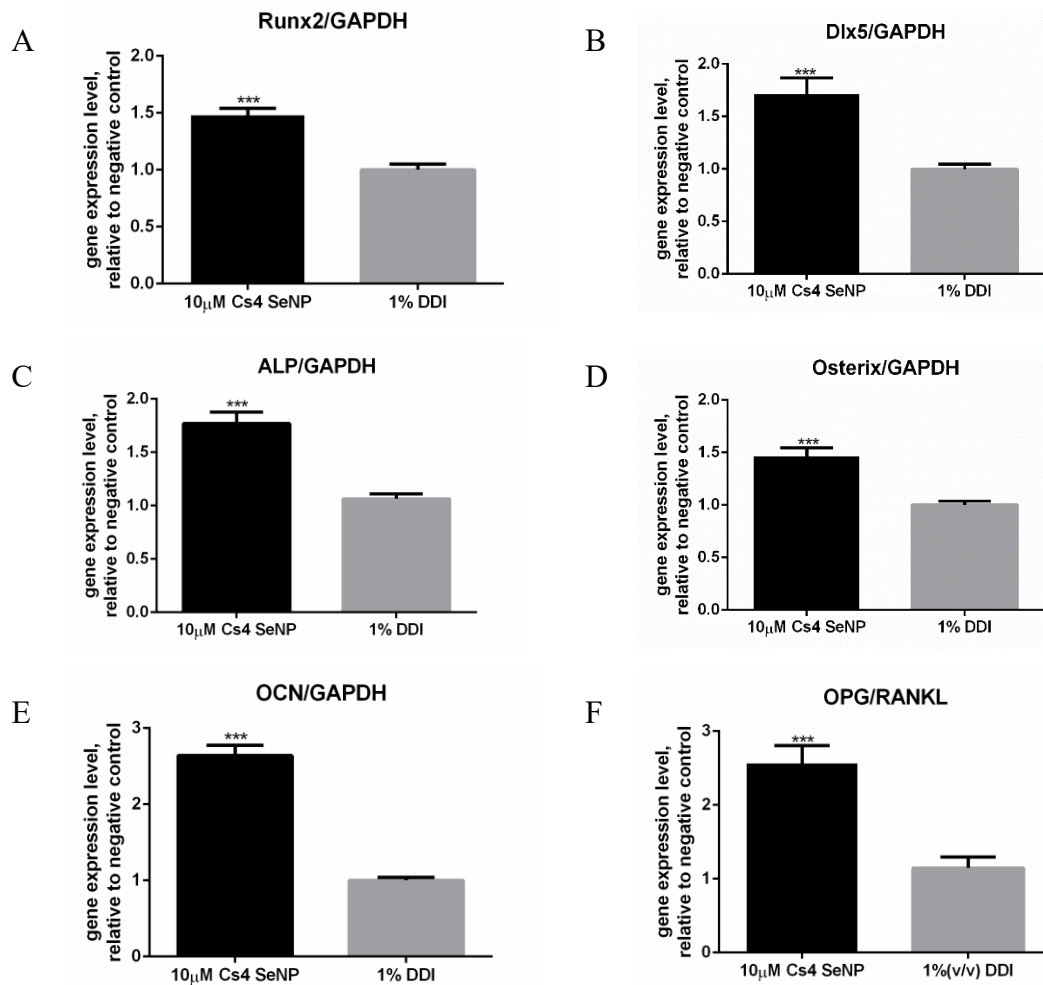
Figure 11. Cs4-SeNPs upregulated the major osteogenic markers in MC3T3-E1 cells during osteoblastic differentiation and mineralization.

Gene expression of (A) Runx2, (B) Dlx5, (C) ALP, (D) Osx, (E) OCN, (F) OPG/RANKL in MC3T3-E1 cells pre-treated with 10μM of Cs4-SeNPs or 1% (v/v) DDI for 6 (Runx2, Dlx5, ALP, Osx, OPG/ RANKL) and 9 days (OCN) was quantified by qPCR analysis and normalized to that of GAPDH. Results are mean values of three determinations ± SEM. Means with "***" are significantly different ($p < 0.001$; Student's *t*-test).

3.2.3 BMP-2 Signaling Cascades Modulated by Cs4-SeNPs in MC3T3-E1 Cells During

Osteoblastic Differentiation

Substantial evidences have demonstrated that BMP-2 signaling via Smad-

dependent and/or Smad-independent pathway(s) is one the most important signaling

cascades in regulating osteoblastogenesis [30-32]. In Smad-dependent pathway, upon cell

surface ligand binding, BMP-2 forms a hetero-tetrameric receptor complex with the

dimers of both type II and type I transmembrane serine/threonine kinases, triggering

phosphorylation of Smad1/5/8 in the cytoplasm. Phosphorylated Smad1/5/8 then forms

a trimetric complex with Smad4 followed by translocation to nucleus, where they

regulate the transcription of target genes for osteoblast differentiation. In particular,

homeobox gene Dlx5, which is an upstream target of both BMP-2/Smad dependent and

BMP-2/Smad independent pathways, plays a pivotal role in stimulating the downstream

transcription factors such as Runx2 and Osx at late differentiation stage [98]. MAPKs

(including p38, ERK and JNK) signaling, which are upstream regulators of Dlx5 in the

BMP-2/Smad independent pathway, has been found to play important role in osteoblast

differentiation, regulating the ALP, Runx2 and OCN expressions [28]. Interestingly, we

discovered that Cs4-SeNPs (10μM) not only significantly upregulated the gene

expression of Dxl5 (1.71 ± 0.15 folds) but also markedly increased the protein

expression of BMP-2 (1.46 ± 0.06 folds) as well as phosphorylation of Smad1/5/8 (2.00

± 0.25 folds) and p38 (1.60 ± 0.10 folds) (**Figure 12Figure** 13**Figure** 14**)**. The

involvement of BMP-2/Smad dependent pathway in SeNPs (functionalized by ruthenium and citrate) mediated osteoblast differentiation has been reported recently [99]. Surprisingly, our findings suggest that Cs4-SeNPs could trigger both BMP-2/Smad-dependent and Smad-independent pathways in the MC3T3-E1 cells during osteoblast differentiation. The proposed BMP-2 signaling cascades modulated by Cs4-SeNPs in the MC3T3 E-1 cells during osteoblast differentiation is shown in **Figure 15**. Nevertheless, after cellular internalization, the specific role of Cs4-SeNPs in regulating osteoblastogenesis of MC3T3 E-1 cells via BMP-2/Smad dependent and independent pathways is not clear at this stage.
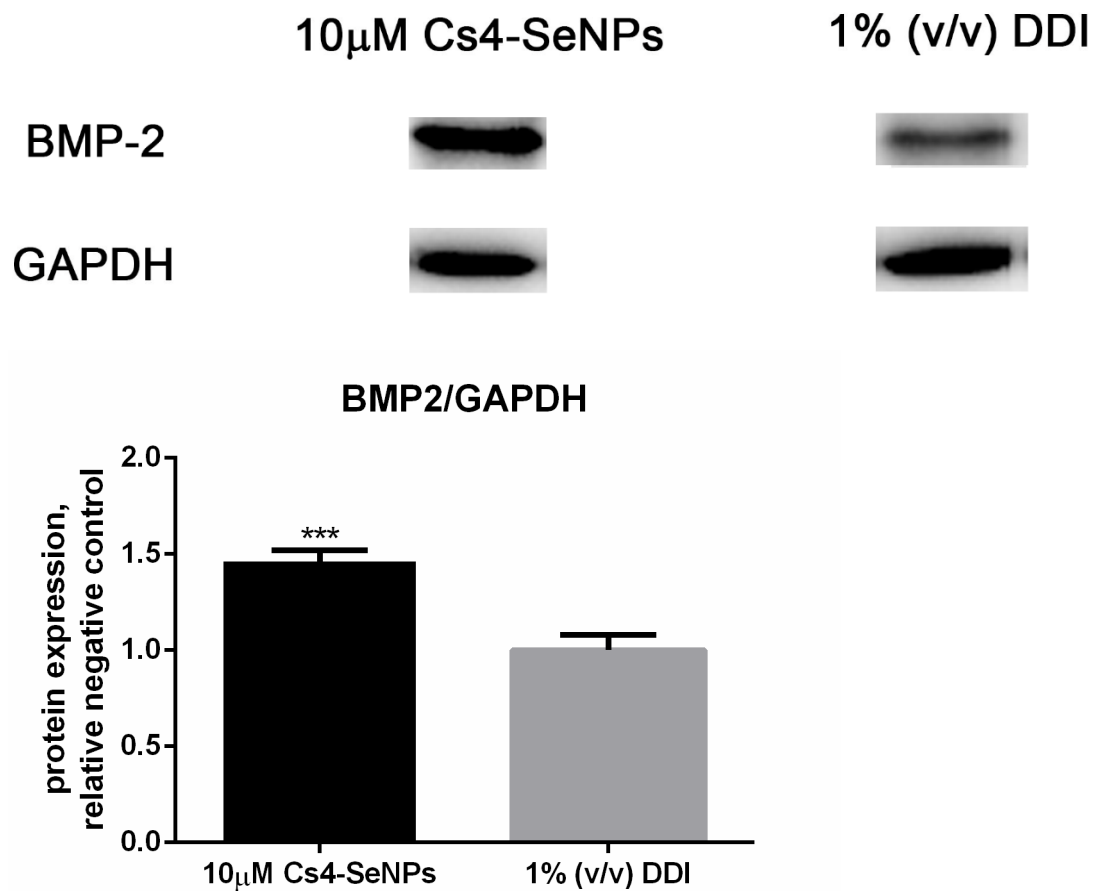
Figure 12. Cs4-SeNPs upregulated the BMP-2 protein expression

Protein expression of BMP-2 in MC3T3-E1 cells pre-treated with 10μM of Cs4-SeNPs or 1% (v/v) DDI for 3 days was quantified by Western blot analysis and normalized to that of GAPDH. Semi-quantification of images was obtained by ImageJ. Results are mean values of three determinations ± SEM. Means with "***" are significantly different ($p < 0.001$; Student's t test).
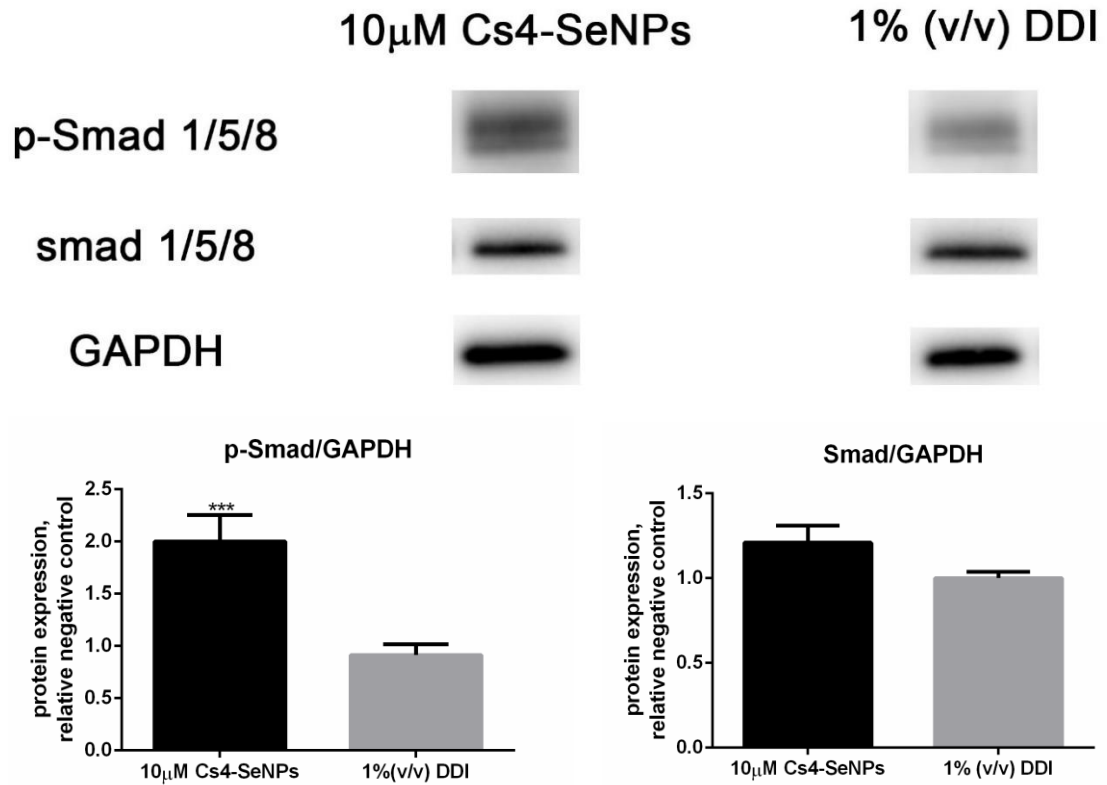
Figure 13. Cs4-SeNPs induced the BMP-2/Smad dependent pathway

Protein expression and phosphorylation of Smad 1/5/8 in MC3T3-E1 cells pre-treated with 10μM of Cs4-SeNPs or 1% (v/v) DDI for 3 days was quantified by Western blot analysis and normalized to that of GAPDH. Semi-quantification of images was obtained by ImageJ. Results are mean values of three determinations ± SEM. Means with "***" are significantly different ($p < 0.001$; Student's t test).

A

10μM Cs4-SeNPs   **1% (v/v) DDI**

p-p38

p38

GAPDH

p-p38/GAPDH

p38/GAPDH

B

10μM Cs4-SeNPs   **1% (v/v) DDI**

p-ERK

ERK

GAPDH

p-ERK/GAPDH

ERK/GAPDH

Figure 14. Cs4-SeNPs induced the BMP-2/Smad independent pathway in MC3T3-E1 cells.

Protein expression and phosphorylation of (A) p38, (B) ERK and (C) JNK in MC3T3-E1 cells pre-treated with 10μM of Cs4-SeNPs or 1% (v/v) DDI for 3 days was quantified by Western blot analysis and normalized to that of GAPDH. Semi-quantification of images was obtained by ImageJ. Results are mean values of three determinations ± SEM. Means with "**" are significantly different ($p < 0.001$; Student's *t* test).
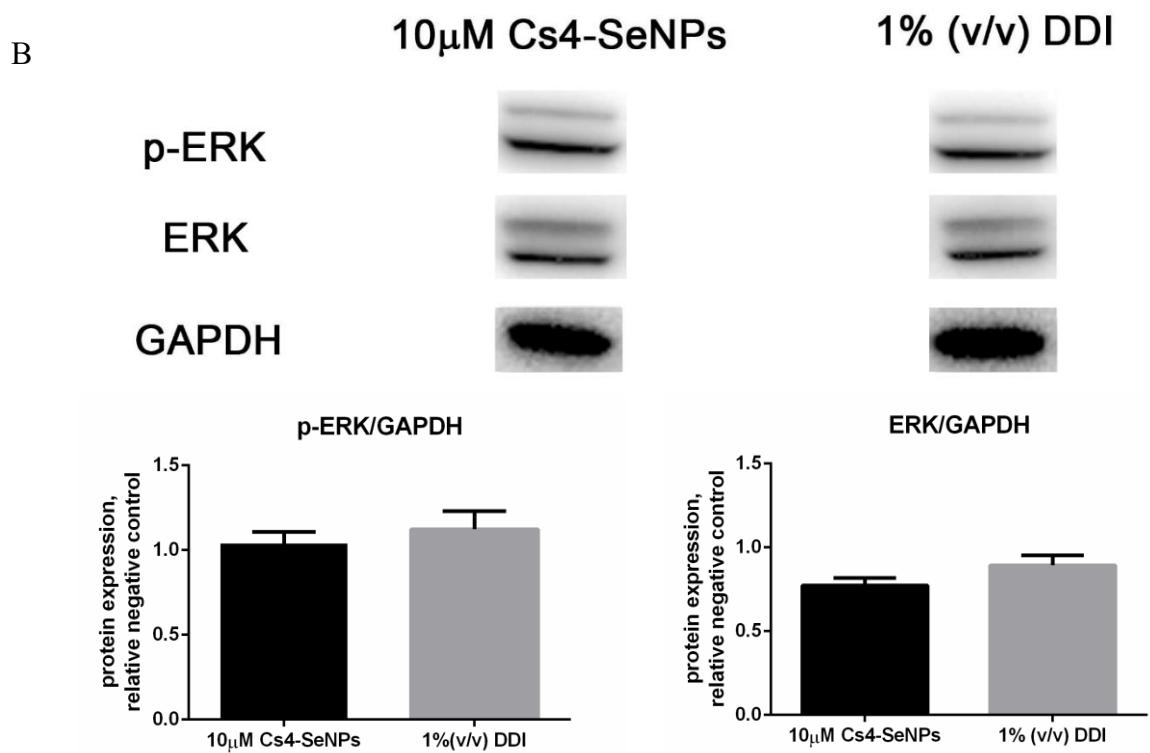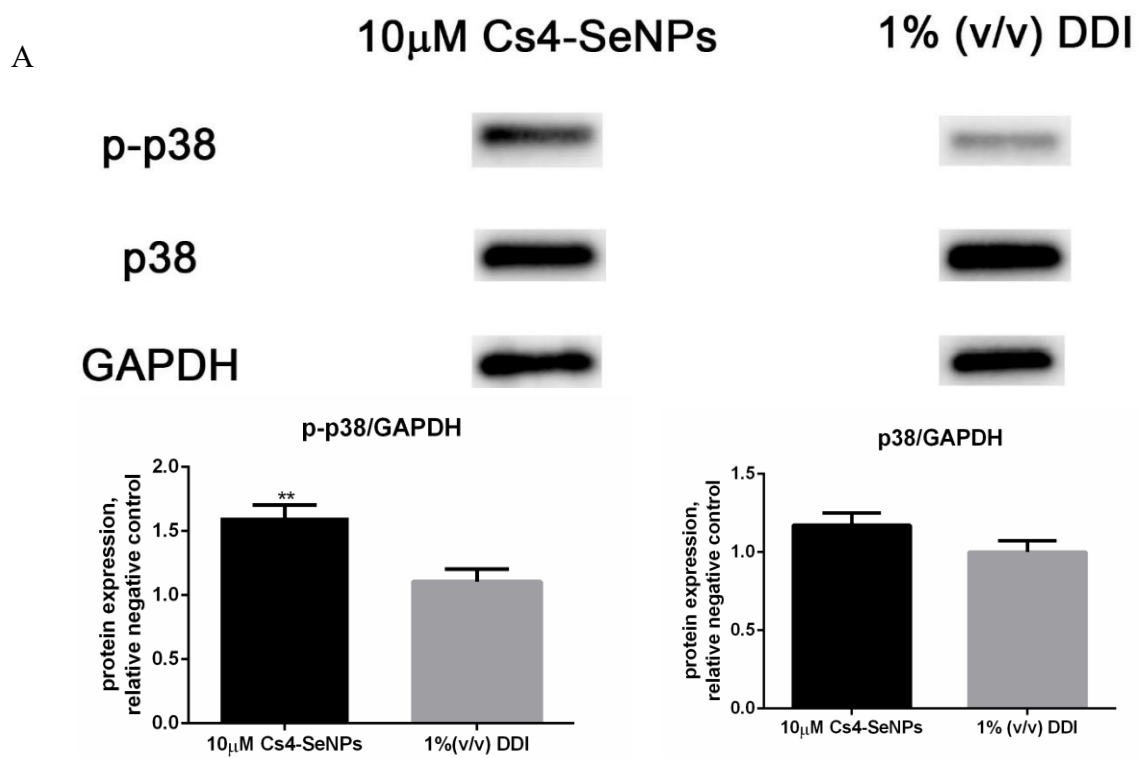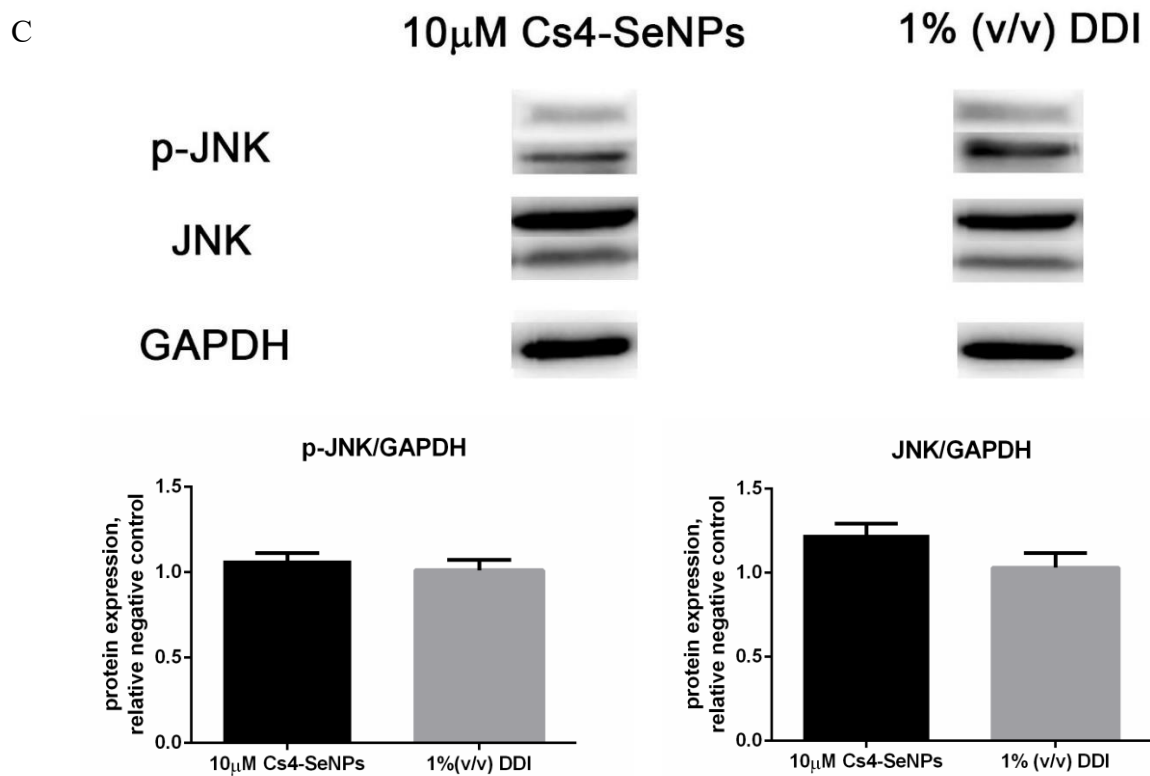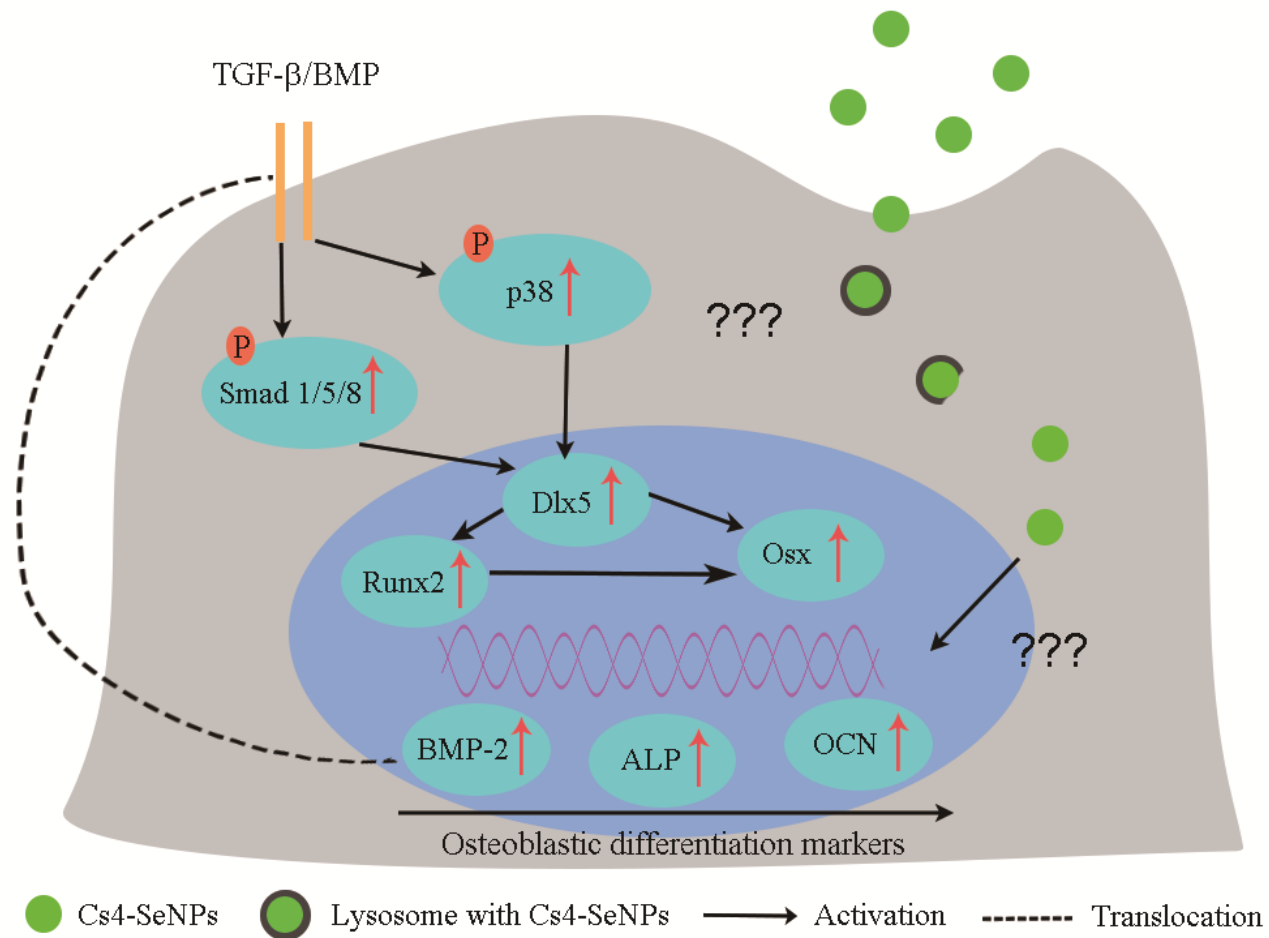
Figure 15. Proposed BMP-2 signaling pathway mediated by Cs4-SeNPs in MC3T3-E1 cells during osteoblastic differentiation

3.3 Cellular Uptake Behavior of Cs4-SeNPs by MC3T3-E1 Cells

Endocytosis has been widely reported as the major cellular uptake mechanism for nanoparticles [100] and lysosomes are major cell organelles responsible for enzymatic digestion of external biomolecules during endocytosis. As shown in **Figure 16**, the overlay of the blue (nucleus), green (Cs4-SeNPs) and red (lysosomes) fluorescence clearly indicated the co-localization of Cs4-SeNPs (10μM) and lysosomes in the MC3T3-E1 cells occurred as early as 12 min, strongly suggesting that Cs4-SeNPs was uptaken by MC3T3-E1 cells via endocytosis and lysosome is the main target organelle. Interestingly, previous studies have reported that both size and shape of nanoparticles are crucial for its cellular uptake efficiency and kinetics. A spherical nanoparticle exhibited a better and quicker cellular internalization during endocytosis. Besides, cells could more easily form a vesicle for one nanoparticle with a size of less than 100nm, since this size is able to gather the nearby receptors on cell surface without binding with other nanoparticles [101]. Thus, in the present study, the relatively rapid cellular uptake of Cs4-SeNPs by MC3T3-E1 cells might be attributed to its spherical shape with a size of 73.2 ± 3.49 nm (**Figure 4**).

Phase Contrast	Nucleus (Hoechst)	Lysosome (Lysotracker)	Cs4-SeNPs (Coumarin-6)	Overlay
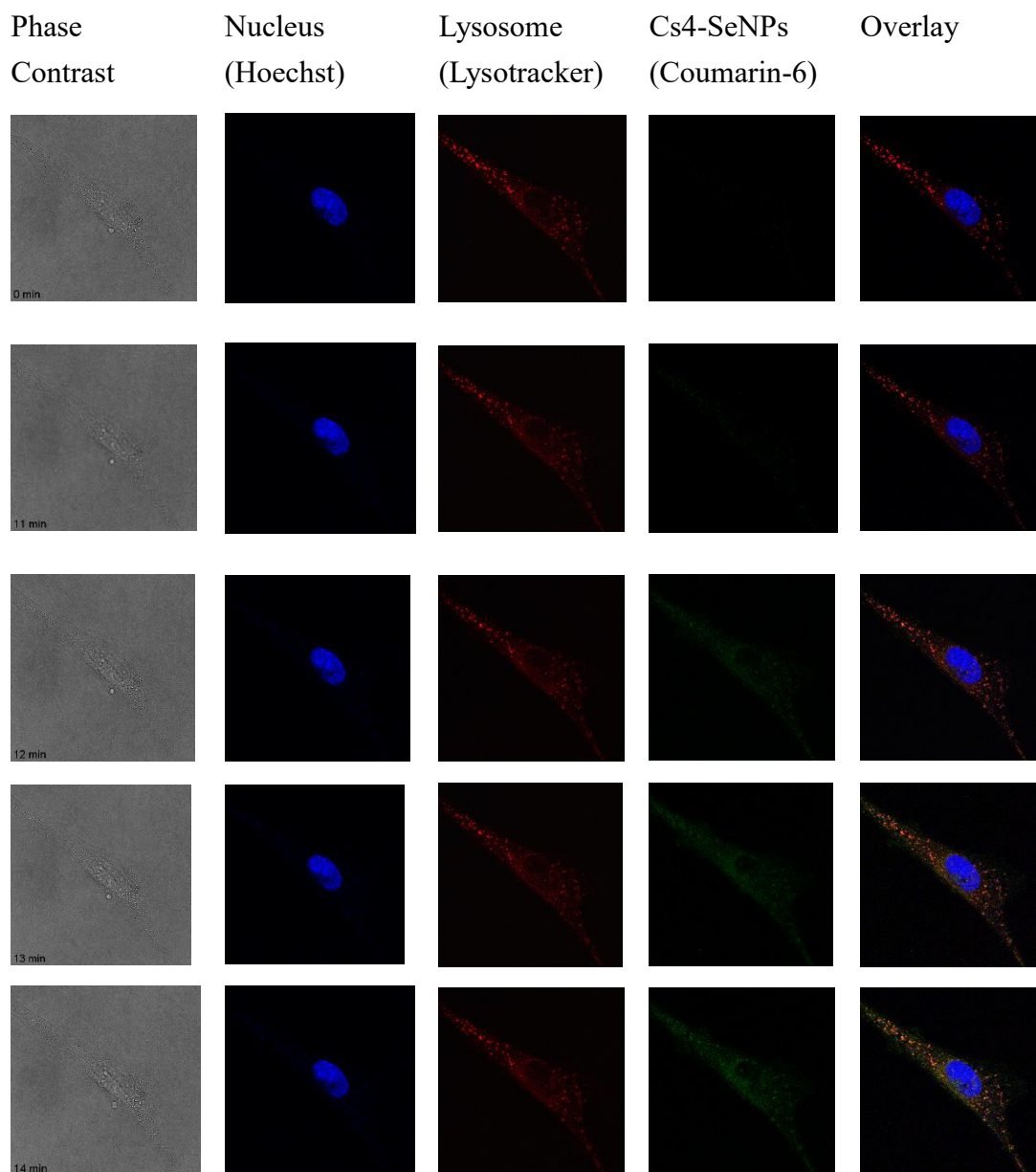
Figure 16. Cs4-SeNPs co-localized with lysosomes in the MC3T3-E1 cells after cellular internalization.

Cells were pre-treated with Hoechst 33342 (blue; nucleus), LysoTracker Deep Red (Red; lysosomes) and courmarin-6-loaded Cs4-SeNPs (10µM; green) at 37 °C for different period of time followed by visualization under fluorescence microscope (Scale bar: 20µm).

4.   Conclusion

4.1 <u>Conclusion</u>

By using the mushroom polysaccharide isolated from *Cordyceps sinensis*, we have successfully prepared novel SeNPs (Cs4-SeNPs) under a simple, food grade redox system. Cs4-SeNPs existed as well-dispensed spherical particles in water with an average diameter of 73.2 ± 3.49nm, possessing a polycrystalline structure with high level of Se (83.9%). X-ray Diffraction (XRD) is a versatile technique that can investigate more degree of diffraction than conventional SAED-TEM [102] and is commonly used in crystallography analysis for studying lattice structure and orientation of inorganic nano-compounds [103-104]. Further characterization using XRD would allow to provide a clearer crystal structure of the Cs4-SeNPs.

Substantial previous findings have demonstrated that promoting bone formation is one of the effective strategies to prevent and/or manage postmenopausal osteoporosis. Interestingly, unlike the common food source of organic (e.g. selenomethionine) and inorganic selenocompounds (e.g. selenite), our study indicated that Cs4-SeNPs (10μM) not only promoted osteoblastogenesis (including cell proliferation, osteogenic differentiation and bone mineral formation), but also indirectly inhibited osteoclastogenesis in the murine preosteoblast MC3T3-E1 cells mediated by both BMP-2/Smad dependent and independent pathways. Thus, it would be interesting to

further characterize their direct effects on osteogenesis using different cell stages of human osteoblasts such as human bone marrow-derived mesenchymal stem cells and hFOB 1.19 human fetal osteoblast cells as well as studying the effects of Cs4-SeNPs on osteoclastogenesis on osteoclasts such as RAW 264.7 cells. In addition, it is interested to study the role of Noggin (Smad inhibitor) and p38 MAP kinase inhibitor on osteoblastogenesis to further confirm the Smad dependent and independent pathways exhibited by Cs4-SeNPs. Besides, verification and validation of the findings with widely used animal models such as mice or rats are also essential to study the bone protective effects by Cs4-SeNPs such as MicroCT study on BMD and microarchitecture and study of protein and gene expression of major biomarkers in bone remodeling.

Endocytosis has been widely reported as the major cellular uptake mechanism for nanoparticles. Cs4-SeNPs ($10\mu M$) was found to co-localize with the lysosomes in the MC3T3-E1 cells as early as 12 min after cellular internalization. Further elucidation of the molecular mechanism of Cs4-SeNPs induced endocytosis is highly valuable.

Our long-term goal is to develop Cs4-SeNPs into an evidence-based bone-forming agent for promoting the bone health of postmenopausal patients in local community.

# 5.	References

1. Väänänen, H. K.; Härkönen, P. L., Estrogen and bone metabolism. *Maturitas* **1996,** *23*, S65-S69.

2. Mithal, A.; Ebeling, P. Asia-Pacific Regional Audit: Epidemiology, costs and burden of osteoporosis 2013. https://www.iofbonehealth.org/sites/default/files/media/PDFs/Regional%20Audits/2013-Asia_Pacific_Audit_0_0.pdf (accessed July 13, 2017).

3. Manolagas, S. C., Birth and death of bone cells: basic regulatory mechanisms and implications for the pathogenesis and treatment of osteoporosis 1. *Endocrine reviews* **2000,** *21* (2), 115-137.

4. Kanis, J. A.; Melton, L. J.; Christiansen, C.; Johnston, C. C.; Khaltaev, N., The diagnosis of osteoporosis. *Journal of bone and mineral research* **1994,** *9* (8), 1137-1141.

5. Young, R., 2013 OSHK guideline for clinical management of postmenopausal osteoporosis in Hong Kong preface. Hong Kong Medical Journal: 2013; Vol. 19.

6. Woo, S.-B.; Hellstein, J. W.; Kalmar, J. R., Systematic review: bisphosphonates and osteonecrosis of the jaws. *Annals of Internal Medicine* **2006,** *144* (10), 753-761.

7. Kyrgidis, A.; Toulis, K., Denosumab-related osteonecrosis of the jaws. *Osteoporos Int* **2011,** *22* (1), 369-370.

8. Dubik, D.; Dembinski, T. C.; Shiu, R. P. C., Stimulation of c-myc oncogene expression associated with estrogen-induced proliferation of human breast cancer cells. *Cancer Research* **1987,** *47* (24 Part 1), 6517-6521.

9. Grumbach Melvin, M., Estrogen, bone, growth and sex: a sea change in conventional wisdom. In *Journal of Pediatric Endocrinology and Metabolism*, 2000; Vol. 13, p 1439.

10. Writing Group for the Women's Health Initiative, I., Risks and benefits of estrogen plus progestin in healthy postmenopausal women: Principal results from the women's health initiative randomized controlled trial. *Journal of the American Medical Association* **2002,** *288* (3), 321-333.

11. Million Women Study, C., Breast cancer and hormone-replacement therapy in the Million Women Study. *The Lancet* **2003,** *362* (9382), 419-427.

12. Heckbert, S. R.; Li, G.; Cummings, S. R.; Smith, N. L.; Psaty, B. M., Use of alendronate and risk of incident atrial fibrillation in women. *Archives of internal medicine* **2008,** *168* (8), 826-31.

13. Cummings, S. R.; San Martin, J.; McClung, M. R.; Siris, E. S.; Eastell, R.; Reid, I. R.; Delmas, P.; Zoog, H. B.; Austin, M.; Wang, A.; Kutilek, S.; Adami, S.; Zanchetta, J.; Libanati, C.; Siddhanti, S.; Christiansen, C., Denosumab for prevention of fractures in postmenopausal women with osteoporosis. *The New England journal of medicine* **2009,** *361* (8), 756-65.

14. Chawla, S.; Henshaw, R.; Seeger, L.; Choy, E.; Blay, J. Y.; Ferrari, S.; Kroep, J.; Grimer, R.; Reichardt, P.; Rutkowski, P.; Schuetze, S.; Skubitz, K.; Staddon, A.; Thomas, D.; Qian, Y.; Jacobs, I., Safety and efficacy of denosumab for adults and skeletally mature adolescents with giant cell tumour of bone: interim analysis of an open-label, parallel-group, phase 2 study. *The Lancet Oncology* **2013,** *14* (9), 901-8.

15. Marx, R. E.; Sawatari, Y.; Fortin, M.; Broumand, V., Bisphosphonate-induced exposed bone (osteonecrosis/osteopetrosis) of the jaws: risk factors, recognition, prevention, and treatment. *Journal of Oral and Maxillofacial Surgery* **2005,** *63* (11), 1567-75.

16. Marx, R. E.; Cillo, J. E., Jr.; Ulloa, J. J., Oral bisphosphonate-induced

osteonecrosis: risk factors, prediction of risk using serum CTX testing, prevention, and treatment. *Journal of Oral and Maxillofacial Surgery* **2007,** *65* (12), 2397-410.

17. Abrahamsen, B.; Eiken, P.; Brixen, K., Atrial fibrillation in fracture patients treated with oral bisphosphonates. *Journal of internal medicine* **2009,** *265* (5), 581-92.

18. McClung, M. R.; Lewiecki, E. M.; Cohen, S. B.; Bolognese, M. A.; Woodson, G. C.; Moffett, A. H.; Peacock, M.; Miller, P. D.; Lederman, S. N.; Chesnut, C. H.; Lain, D.; Kivitz, A. J.; Holloway, D. L.; Zhang, C.; Peterson, M. C.; Bekker, P. J., Denosumab in postmenopausal women with low bone mineral density. *The New England journal of medicine* **2006,** *354* (8), 821-31.

19. Deeks, E. D.; Dhillon, S., Strontium ranelate: a review of its use in the treatment of postmenopausal osteoporosis. *Drugs* **2010,** *70* (6), 733-59.

20. Notelovitz, M., Estrogen therapy and osteoporosis: principles & practice. *The American Journal of the Medical Sciences* **1997,** *313* (1), 2-12.

21. Reginster, J. Y.; Felsenberg, D.; Boonen, S.; Diez-Perez, A.; Rizzoli, R.; Brandi, M. L.; Spector, T. D.; Brixen, K.; Goemaere, S.; Cormier, C.; Balogh, A.; Delmas, P. D.; Meunier, P. J., Effects of long-term strontium ranelate treatment on the risk of nonvertebral and vertebral fractures in postmenopausal osteoporosis: Results of a five-year, randomized, placebo-controlled trial. *Arthritis & Rheumatism* **2008,** *58* (6), 1687-1695.

22. Cauley, J. A.; Robbins, J.; Chen, Z.; Cummings, S. R.; Jackson, R. D.; LaCroix, A. Z.; LeBoff, M.; Lewis, C. E.; McGowan, J.; Neuner, J.; Pettinger, M.; Stefanick, M. L.; Wactawski-Wende, J.; Watts, N. B.; Investigators, W. s. H. I., Effects of estrogen plus progestin on risk of fracture and bone mineral density: the Women's Health

Initiative randomized trial. *JAMA* **2003,** *290* (13), 1729-38.

23. Beral, V.; Collaborators, M. W. S., Breast cancer and hormone-replacement therapy in the Million Women Study. *The Lancet* **2003,** *362* (9382), 419-427.

24. Meunier, P. J.; Roux, C.; Ortolani, S.; Diaz-Curiel, M.; Compston, J.; Marquis, P.; Cormier, C.; Isaia, G.; Badurski, J.; Wark, J. D.; Collette, J.; Reginster, J. Y., Effects of long-term strontium ranelate treatment on vertebral fracture risk in postmenopausal women with osteoporosis. *Osteoporos Int* **2009,** *20* (10), 1663-73.

25. Bjarnason, N. H.; Hassager, C.; Christiansen, C., Postmenopausal bone remodelling and hormone replacement. *Climacteric : the journal of the International Menopause Society* **1998,** *1* (1), 72-9.

26. Hadjidakis, D. J.; Androulakis, I. I., Bone Remodeling. *Annals of the New York Academy of Sciences* **2006,** *1092* (1), 385-396.

27. Pittenger, M. F.; Mackay, A. M.; Beck, S. C.; Jaiswal, R. K.; Douglas, R.; Mosca, J. D.; Moorman, M. A.; Simonetti, D. W.; Craig, S.; Marshak, D. R., Multilineage potential of adult human mesenchymal stem cells. *Science* **1999,** *284* (5411), 143-147.

28. Huang, W.; Yang, S.; Shao, J.; Li, Y.-P., Signaling and transcriptional regulation in osteoblast commitment and differentiation. *Frontiers in Bioscience: a Journal and Virtual Library* **2007,** *12*, 3068.

29. Marie, P. J.; Fromigué, O.; Modrowski, D., Deregulation of osteoblast differentiation in primary bone cancers In *Bone Cancer (Second edition)*, Academic Press: San Diego, 2015; pp 39-54.

30. Canalis, E.; Economides, A. N.; Gazzerro, E., Bone morphogenetic proteins, their antagonists, and the skeleton. *Endocrine Reviews* **2003,** *24* (2), 218-35.

31. Chen, D.; Zhao, M.; Mundy, G. R., Bone morphogenetic proteins. *Growth factors (Chur, Switzerland)* **2004,** *22* (4), 233-41.

32. Cao, X.; Chen, D., The BMP signaling and in vivo bone formation. *Gene* **2005,** *357* (1), 1-8.

33. Anderson, H. C.; Hodges, P. T.; Aguilera, X. M.; Missana, L.; Moylan, P. E., Bone morphogenetic protein (BMP) localization in developing human and rat growth plate, metaphysis, epiphysis, and articular cartilage. *Journal of Histochemistry and Cytochemistry* **2000,** *48* (11), 1493-502.

34. Daluiski, A.; Engstrand, T.; Bahamonde, M. E.; Gamer, L. W.; Agius, E.; Stevenson, S. L.; Cox, K.; Rosen, V.; Lyons, K. M., Bone morphogenetic protein-3 is a negative regulator of bone density. *Nature genetics* **2001,** *27* (1), 84-8.

35. Derynck, R.; Akhurst, R. J.; Balmain, A., TGF-beta signaling in tumor suppression and cancer progression. *Nature genetics* **2001,** *29* (2), 117-29.

36. Massague, J., How cells read TGF-beta signals. *Nature Reviews Molecular Cell Biology* **2000,** *1* (3), 169-78.

37. Zhang, Y. W.; Yasui, N.; Ito, K.; Huang, G.; Fujii, M.; Hanai, J.; Nogami, H.; Ochi, T.; Miyazono, K.; Ito, Y., A RUNX2/PEBP2alpha A/CBFA1 mutation displaying impaired transactivation and Smad interaction in cleidocranial dysplasia. *Proceedings of the National Academy of Sciences* **2000,** *97* (19), 10549-54.

38. Miyazono, K.; Maeda, S.; Imamura, T., Coordinate regulation of cell growth and differentiation by TGF-beta superfamily and Runx proteins. *Oncogene* **2004,** *23* (24), 4232-7.

39. Ito, Y.; Miyazono, K., RUNX transcription factors as key targets of TGF-beta superfamily signaling. *Current opinion in genetics & development* **2003,** *13* (1), 43-7.

40. Miyama, K.; Yamada, G.; Yamamoto, T. S.; Takagi, C.; Miyado, K.; Sakai, M.; Ueno, N.; Shibuya, H., A BMP-inducible gene, dlx5, regulates osteoblast differentiation and mesoderm induction. *Developmental biology* **1999,** *208* (1), 123-33.

41. Lee, M. H.; Kim, Y. J.; Kim, H. J.; Park, H. D.; Kang, A. R.; Kyung, H. M.; Sung, J. H.; Wozney, J. M.; Ryoo, H. M., BMP-2-induced Runx2 expression is mediated by Dlx5, and TGF-beta 1 opposes the BMP-2-induced osteoblast differentiation by suppression of Dlx5 expression. *Journal of Biological Chemistry* **2003,** *278* (36), 34387-94.

42. de Jong, D. S.; Vaes, B. L.; Dechering, K. J.; Feijen, A.; Hendriks, J. M.; Wehrens, R.; Mummery, C. L.; van Zoelen, E. J.; Olijve, W.; Steegenga, W. T., Identification of novel regulators associated with early-phase osteoblast differentiation. *Journal of Bone and Mineral Research* **2004,** *19* (6), 947-58.

43. Korchynskyi, O.; Dechering, K. J.; Sijbers, A. M.; Olijve, W.; ten Dijke, P., Gene array analysis of bone morphogenetic protein type I receptor-induced osteoblast differentiation. *Journal of Bone and Mineral Research* **2003,** *18* (7), 1177-85.

44. Guicheux, J.; Lemonnier, J.; Ghayor, C.; Suzuki, A.; Palmer, G.; Caverzasio, J., Activation of p38 mitogen-activated protein kinase and c-Jun-NH2-terminal kinase by BMP-2 and their implication in the stimulation of osteoblastic cell differentiation. *Journal of Bone and Mineral Research* **2003,** *18* (11), 2060-8.

45. Lai, C. F.; Cheng, S. L., Signal transductions induced by bone morphogenetic protein-2 and transforming growth factor-beta in normal human osteoblastic cells. *Journal of Biological Chemistry* **2002,** *277* (18), 15514-22.

46. Lemonnier, J.; Ghayor, C.; Guicheux, J.; Caverzasio, J., Protein kinase C-independent activation of protein kinase D is involved in BMP-2-induced

activation of stress mitogen-activated protein kinases JNK and p38 and osteoblastic cell differentiation. *Journal of Biological Chemistry* **2004,** *279* (1), 259-64.

47. Lee, K. S.; Hong, S. H.; Bae, S. C., Both the Smad and p38 MAPK pathways play a crucial role in Runx2 expression following induction by transforming growth factor-beta and bone morphogenetic protein. *Oncogene* **2002,** *21* (47), 7156-63.

48. Lee, K. S.; Kim, H. J.; Li, Q. L.; Chi, X. Z.; Ueta, C.; Komori, T.; Wozney, J. M.; Kim, E. G.; Choi, J. Y.; Ryoo, H. M.; Bae, S. C., Runx2 is a common target of transforming growth factor beta1 and bone morphogenetic protein 2, and cooperation between Runx2 and Smad5 induces osteoblast-specific gene expression in the pluripotent mesenchymal precursor cell line C2C12. *Molecular and cellular biology* **2000,** *20* (23), 8783-92.

49. Lee, M. H.; Javed, A.; Kim, H. J.; Shin, H. I.; Gutierrez, S.; Choi, J. Y.; Rosen, V.; Stein, J. L.; van Wijnen, A. J.; Stein, G. S.; Lian, J. B.; Ryoo, H. M., Transient upregulation of CBFA1 in response to bone morphogenetic protein-2 and transforming growth factor beta1 in C2C12 myogenic cells coincides with suppression of the myogenic phenotype but is not sufficient for osteoblast differentiation. *Journal of cellular biochemistry* **1999,** *73* (1), 114-25.

50. Nakashima, K.; Zhou, X.; Kunkel, G.; Zhang, Z.; Deng, J. M.; Behringer, R. R.; de Crombrugghe, B., The novel zinc finger-containing transcription factor osterix is required for osteoblast differentiation and bone formation. *Cell* **2002,** *108* (1), 17-29.

51. Yagi, K.; Tsuji, K.; Nifuji, A.; Shinomiya, K.; Nakashima, K.; DeCrombrugghe, B.; Noda, M., Bone morphogenetic protein-2 enhances osterix gene expression in chondrocytes. *Journal of cellular biochemistry* **2003,** *88* (6), 1077-83.

52. Lee, M. H.; Kwon, T. G.; Park, H. S.; Wozney, J. M.; Ryoo, H. M., BMP-2-induced Osterix expression is mediated by Dlx5 but is independent of Runx2. *Biochemical and Biophysical Research Communications* **2003,** *309* (3), 689-94.

53. Celil, A. B.; Hollinger, J. O.; Campbell, P. G., Osx transcriptional regulation is mediated by additional pathways to BMP2/Smad signaling. *Journal of Cellular Biochemistry* **2005,** *95* (3), 518-28.

54. Wu, M.; Chen, G.; Li, Y. P., TGF-β and BMP signaling in osteoblast, skeletal development, and bone formation, homeostasis and disease. *Bone Research* **2016,** *4*, 16009.

55. Shore, E. M.; Kaplan, F. S., Inherited human diseases of heterotopic bone formation. *Nature Reviews Rheumatology* **2010,** *6* (9), 518-27.

56. Monsen, E. R., Dietary Reference Intakes for The Antioxidant Nutrients. *Journal of the American Dietetic Association* **2000,** *100* (6), 637-640.

57. Davis, C. D.; Tsuji, P. A.; Milner, J. A., Selenoproteins and Cancer Prevention. *Annu. Rev. Nutr.* **2012,** *32* (1), 73-95.

58. Cao, J. J.; Gregoire, B. R.; Zeng, H., Selenium Deficiency Decreases Antioxidative Capacity and Is Detrimental to Bone Microarchitecture in Mice. *The Journal of Nutrition* **2012,** *142* (8), 1526-1531.

59. Saito, Y.; Yoshida, Y.; Akazawa, T.; Takahashi, K.; Niki, E., Cell Death Caused by Selenium Deficiency and Protective Effect of Antioxidants. *Journal of Biological Chemistry* **2003,** *278* (41), 39428-39434.

60. Zhang, J.; Munger, R. G.; West, N. A.; Cutler, D. R.; Wengreen, H. J.; Corcoran, C. D., Antioxidant Intake and Risk of Osteoporotic Hip Fracture in Utah: An Effect Modified by Smoking Status. *American Journal of Epidemiology* **2006,** *163* (1), 9-17.

61. Rayman, M. P., Selenium and human health. *The Lancet* **2012,** *379* (9822), 1256-1268.

62. Moreno-Reyes, R.; Egrise, D.; Nève, J.; Pasteels, J.-L.; Schoutens, A., Selenium deficiency-induced growth retardation is associated with an impaired bone metabolism and osteopenia. *Journal of Bone and Mineral Research* **2001,** *16* (8), 1556-1563.

63. Moreno-Reyes, R.; Mathieu, F.; Boelaert, M.; Begaux, F.; Suetens, C.; Rivera, M. T.; Nève, J.; Perlmutter, N.; Vanderpas, J., Selenium and iodine supplementation of rural Tibetan children affected by Kashin-Beck osteoarthropathy. *The American Journal of Clinical Nutrition* **2003,** *78* (1), 137-144.

64. Liu, H.; Bian, W.; Liu, S.; Huang, K., Selenium protects bone marrow stromal cells against hydrogen peroxide-induced inhibition of osteoblastic differentiation by suppressing oxidative stress and ERK signaling pathway. *Biological Trace Element Research* **2012,** *150* (1-3), 441-50.

65. Wang, H.; Zhang, J.; Yu, H., Elemental selenium at nano size possesses lower toxicity without compromising the fundamental effect on selenoenzymes: comparison with selenomethionine in mice. *Free Radical Biology & Medicine* **2007,** *42* (10), 1524-33.

66. Yang, F.; Tang, Q.; Zhong, X.; Bai, Y.; Chen, T.; Zhang, Y.; Li, Y.; Zheng, W., Surface decoration by Spirulina polysaccharide enhances the cellular uptake and anticancer efficacy of selenium nanoparticles. *International Journal of Nanomedicine* **2012,** *7*, 835-844.

67. Benko, I.; Nagy, G.; Tanczos, B.; Ungvari, E.; Sztrik, A.; Eszenyi, P.; Prokisch, J.; Banfalvi, G., Subacute toxicity of nano-selenium compared to other selenium species in mice. *Environmental toxicology and chemistry* **2012,** *31* (12), 2812-

2820.

68. Zhang, J.; Wang, H.; Yan, X.; Zhang, L., Comparison of short-term toxicity between nano-Se and selenite in mice. *Life sciences* **2005,** *76* (10), 1099-109.

69. Zhang, W.; Chen, Z.; Liu, H.; Zhang, L.; Gao, P.; Li, D., Biosynthesis and structural characteristics of selenium nanoparticles by Pseudomonas alcaliphila. *Colloids and Surfaces B: Biointerfaces* **2011,** *88* (1), 196-201.

70. Zhang, Y.; Wang, J.; Zhang, L., Creation of highly stable selenium nanoparticles capped with hyperbranched polysaccharide in water. *Langmuir* **2010,** *26* (22), 17617-17623.

71. Kong, L.; Yuan, Q.; Zhu, H.; Li, Y.; Guo, Q.; Wang, Q.; Bi, X.; Gao, X., The suppression of prostate LNCaP cancer cells growth by Selenium nanoparticles through Akt/Mdm2/AR controlled apoptosis. *Biomaterials* **2011,** *32* (27), 6515-6522.

72. Wu, H.; Zhu, H.; Li, X.; Liu, Z.; Zheng, W.; Chen, T.; Yu, B.; Wong, K.-H., Induction of apoptosis and cell cycle arrest in A549 human lung adenocarcinoma cells by surface-capping selenium nanoparticles: an effect enhanced by polysaccharide–protein complexes from polyporus rhinocerus. *Journal of Agricultural and Food Chemistry* **2013,** *61* (41), 9859-9866.

73. Chen, T.; Wong, Y. S.; Zheng, W.; Bai, Y.; Huang, L., Selenium nanoparticles fabricated in Undaria pinnatifida polysaccharide solutions induce mitochondria-mediated apoptosis in A375 human melanoma cells. *Colloids and Surfaces B: Biointerfaces* **2008,** *67* (1), 26-31.

74. Zhu, J. S.; Halpern, G. M.; Jones, K., The scientific rediscovery of an ancient Chinese herbal medicine: Cordyceps sinensis: part I. *Journal of alternative and complementary medicine (New York, N.Y.)* **1998,** *4* (3), 289-303.

75. Zhou, X.-W.; Li, L.-J.; Tian, E.-W., Advances in research of the artificial cultivation of Ophiocordyceps sinensis in China. *Critical Reviews in Biotechnology* **2014,** *34* (3), 233-243.

76. Cheung, W. M.; Ng, W. W.; Kung, A. W., Dimethyl sulfoxide as an inducer of differentiation in preosteoblast MC3T3-E1 cells. *FEBS letters* **2006,** *580* (1), 121-6.

77. Singha, U. K.; Jiang, Y.; Yu, S.; Luo, M.; Lu, Y.; Zhang, J.; Xiao, G., Rapamycin inhibits osteoblast proliferation and differentiation in MC3T3-E1 cells and primary mouse bone marrow stromal cells. *Journal of cellular biochemistry* **2008,** *103* (2), 434-446.

78. Yazid, M. D.; Ariffin, S. H. Z.; Senafi, S.; Razak, M. A.; Wahab, R. M. A., Determination of the differentiation capacities of murines' primary mononucleated cells and MC3T3-E1 cells. *Cancer Cell International* **2010,** *10* (1), 1.

79. Kokkonen, H. E.; Ilvesaro, J. M.; Morra, M.; Schols, H. A.; Tuukkanen, J., Effect of modified pectin molecules on the growth of bone cells. *Biomacromolecules* **2007,** *8* (2), 509-515.

80. Zheng, C.; Wang, J.; Liu, Y.; Yu, Q.; Liu, Y.; Deng, N.; Liu, J., Functional Selenium Nanoparticles Enhanced Stem Cell Osteoblastic Differentiation through BMP Signaling Pathways, Advanced Functional Materials Volume 24, Issue 43. *Advanced Functional Materials* **2014,** *24* (43), 6872-6883.

81. Ekkapongpisit, M.; Giovia, A.; Follo, C.; Caputo, G.; Isidoro, C., Biocompatibility, endocytosis, and intracellular trafficking of mesoporous silica and polystyrene nanoparticles in ovarian cancer cells: effects of size and surface charge groups. *International Journal of Nanomedicine* **2012,** *7*, 4147-4158.

82. Egerton, R. F., an introduction to TEM, SEM, and AEM. In *Physical principles of electron microscopy*, 1 ed.; Springer Science & Business Media: U.S., 2005; p 210.

83. Horikoshi, S.; Serpone, N., Introduction to Nanoparticles. In *Microwaves in Nanoparticle Synthesis*, Satoshi Horikoshi, N. S., Ed. Wiley-VCH Verlag GmbH & Co. KGaA: 2013; pp 1-24.

84. Filipe, V.; Hawe, A.; Jiskoot, W., Critical Evaluation of Nanoparticle Tracking Analysis (NTA) by NanoSight for the Measurement of Nanoparticles and Protein Aggregates. *Pharmaceutical Research* **2010,** *27* (5), 796-810.

85. Merkus, H. G., *Particle size measurements: fundamentals, practice, quality*. Springer Science & Business Media: 2009; Vol. 17.

86. Wu, H.; Li, X.; Liu, W.; Chen, T.; Li, Y.; Zheng, W.; Man, C. W.-Y.; Wong, M.-K.; Wong, K.-H., Surface decoration of selenium nanoparticles by mushroom polysaccharides-protein complexes to achieve enhanced cellular uptake and antiproliferative activity. *Journal of Materials Chemistry* **2012,** *22* (19), 9602-9610.

87. Berridge, M. V.; Herst, P. M.; Tan, A. S., Tetrazolium dyes as tools in cell biology: new insights into their cellular reduction. *Biotechnology Annual Review* **2005,** *11*, 127-152.

88. Sittampalam, G.; Gal-Edd, N.; Arkin, M., Assay Guidance Manual [Internet]. Bethesda (MD): Eli Lilly & Company and the National Center for Advancing Translational Sciences; 2004. 2012.

89. Vekariya, K. K.; Kaur, J.; Tikoo, K., Alleviating anastrozole induced bone toxicity by selenium nanoparticles in SD rats. *Toxicology and applied pharmacology* **2013,** *268* (2), 212-20.

90. Franceschi, R. T.; Xiao, G., Regulation of the osteoblast-specific transcription factor, Runx2 Responsiveness to multiple signal transduction pathways. *Journal of Cellular Biochemistry* **2003,** *88* (3), 446-454.

91. Komori, T., Regulation of osteoblast differentiation by transcription factors. *Journal of Cellular Biochemistry* **2006,** *99* (5), 1233-1239.

92. Ducy, P.; Zhang, R.; Geoffroy, V.; Ridall, A. L.; Karsenty, G., Osf2/Cbfa1: a transcriptional activator of osteoblast differentiation. *Cell* **1997,** *89* (5), 747-54.

93. Komori, T.; Yagi, H.; Nomura, S.; Yamaguchi, A.; Sasaki, K.; Deguchi, K.; Shimizu, Y.; Bronson, R. T.; Gao, Y. H.; Inada, M.; Sato, M.; Okamoto, R.; Kitamura, Y.; Yoshiki, S.; Kishimoto, T., Targeted disruption of Cbfa1 results in a complete lack of bone formation owing to maturational arrest of osteoblasts. *Cell* **1997,** *89* (5), 755-64.

94. Otto, F.; Thornell, A. P.; Crompton, T.; Denzel, A.; Gilmour, K. C.; Rosewell, I. R.; Stamp, G. W.; Beddington, R. S.; Mundlos, S.; Olsen, B. R.; Selby, P. B.; Owen, M. J., Cbfa1, a candidate gene for cleidocranial dysplasia syndrome, is essential for osteoblast differentiation and bone development. *Cell* **1997,** *89* (5), 765-71.

95. Hofbauer, L.; Kuhne, C.; Viereck, V., The OPG/RANKL/RANK system in metabolic bone diseases. *Journal of Musculoskeletal and Neuronal Interactions* **2004,** *4* (3), 268.

96. Khosla, S., Minireview: The opg/rankl/rank system. *Endocrinology* **2001,** *142* (12), 5050-5055.

97. Zhang, Z.; Zhang, J.; Xiao, J., Selenoproteins and selenium status in bone physiology and pathology. *Biochimica et Biophysica Acta (BBA)-General Subjects* **2014,** *1840* (11), 3246-3256.

98. Huang, W.; Yang, S.; Shao, J.; Li, Y. P., Signaling and transcriptional regulation in

osteoblast commitment and differentiation. *Front Biosci* **2007,** *12*, 3068-92.

99. Zheng, C.; Wang, J.; Liu, Y.; Yu, Q.; Liu, Y.; Deng, N.; Liu, J. Functional Selenium Nanoparticles Enhanced Stem Cell Osteoblastic Differentiation through BMP Signaling Pathways, Advanced Functional Materials Volume 24, Issue 43 *Advanced Functional Materials* [Online], 2014, p. 6872-6883. http://onlinelibrary.wiley.com/doi/10.1002/adfm.201401263/abstract (accessed 01).

100. Ekkapongpisit, M.; Giovia, A.; Follo, C.; Caputo, G.; Isidoro, C., Biocompatibility, endocytosis, and intracellular trafficking of mesoporous silica and polystyrene nanoparticles in ovarian cancer cells: effects of size and surface charge groups. *Int J Nanomedicine* **2012,** *7*, 4147-4158.

101. Shang, L.; Nienhaus, K.; Jiang, X.; Yang, L.; Landfester, K.; Mailänder, V.; Simmet, T.; Nienhaus, G. U., Nanoparticle interactions with live cells: quantitative fluorescence microscopy of nanoparticle size effects. *Beilstein Journal of Nanotechnology* **2014,** *5*, 2388.

102. Chung, F. H., Quantitative interpretation of X-ray diffraction patterns of mixtures. II. Adiabatic principle of X-ray diffraction analysis of mixtures. *Journal of Applied Crystallography* **1974,** *7* (6), 526-531.

103. Zhang, S.-Y.; Zhang, J.; Wang, H.-Y.; Chen, H.-Y., Synthesis of selenium nanoparticles in the presence of polysaccharides. **2004,** *58* (21), 2590-2594.

104. Shin, Y.; Blackwood, J. M.; Bae, I.-T.; Arey, B. W.; Exarhos, G. J., Synthesis and stabilization of selenium nanoparticles on cellulose nanocrystal. **2007,** *61* (21), 4297-4300.